The Dissertation Committee for Li Zhou Certifies that this is the approved version of the following dissertation:

Mechanistic Analysis of Selective Inhibition of RNA Processing in *Escherichia coli*

Committee:

George Georgiou, Supervisor

Vishwanath R Iyer

Edward M. Marcotte

Richard J. Meyer

Ian J. Molineux

Mechanistic Analysis of Selective Inhibition of RNA Processing in *Escherichia coli*

by

Li Zhou, B.S.

Dissertation

Presented to the Faculty of the Graduate School of

The University of Texas at Austin

in Partial Fulfillment

of the Requirements

for the Degree of

Doctor of Philosophy

The University of Texas at Austin

August, 2010

Dedication

To my parents

Acknowledgements

First, I would like to thank my advisor, George Georgiou, for your belief in my ability, optimism, encouragement, support and most importantly, for your patience and guidance in my research. I am grateful to my committee members, Ian Molinuex, Vishwanath Iyer, Richard Meyer and Edward Marcotte for their helpful comments and suggestions.

I would like to thank Meng Zhao for her collaboration in the transcriptional study of *rraA* and *rraB*; I would like to thank Rachel Wolf, David Graham for their assistance in the HPLC analysis. I would like to thank Junjun Gao, Meng Zhao, Chris Liu and Rebecca Cohen for their help in making protein constructs and protein purification. I would like to thank Rong Wang and Christine Vogel for their collaboration on the proteomics study. I would like to thank Teresa Giles, Nandini Aiyappan, Supriya Pai, Everett Stone, and Erik Quandt for proofreading my scientific writings.

I would also like to thank members past and present of Georgiou group for their friendship and help. It is a great experience working with you. In particular, I would like to thank Silvia Arredondo and Mark Pogson for helping with the FPLC, Everett Stone for discussion on kinetic analysis, and Supriya Pai for advices on real time PCR experiments.

Finally, but most of all, I would like to thank my parents for their unconditional love and supports.

Mechanistic Analysis of Selective Inhibition of RNA Processing in *Escherichia coli*

Publication No._____

Li Zhou, PhD

The University of Texas at Austin, 2010

Supervisor: George Georgiou

In *Escherichia coli,* the RNA degradosome is a protein complex involved in the general degradation of mRNA and in post-transcriptional gene regulation. The principal components of the degradosome complex are the endoribonuclease RNase E, the phosphorolytic exoribonuclease PNPase, the ATP-dependent RNA helicase RhlB, and the glycolytic enzyme enolase. The RNase E protein is a 1061 amino acid protein which can be divided into three major functional portions: the N-terminal catalytic activity portion; the central membrane anchoring and RNA binding portion; and the C terminal protein-interaction portion which bind to other major degradosome components.

RraA and RraB (Regulator of RNase E activity) are protein regulators of RNase E discovered in our lab, which regulate RNase E by binding to the RNase E C-terminal region. The work presented here describes the regulation of *rraB* gene expression and *in vitro* studies of degradosome assembly and the effects of RraA/RraB inhibition.

rraB is transcribed from its own promoter P_{rraB}. A transposon insertion into *glmS* encoding glucosamine-6P synthase resulted in a 4 fold increase in the P_{rraB} activity from a P_{rraB}-*lacZ* fusion the indicating that *glmS* is serves as a negative regulator of *rraB* transcription. Consistent with this discovery, real-time RT-PCR revealed that *glmS::*Tn*5* results in a 5-fold increase on the steady-state level of *rraB* mRNA.

As part of this work we have reconstituted the degradosome from individually purified proteins. The binding sites of RraA and RraB overlap with the RNA binding and the RhlB interaction sites within the C-terminus of RNase E. We have characterized the effects of RraA and RraB on the decay of various RNA substrates by reconstituted degradosomes: RraA and RraB proteins were shown to inhibit the hydrolysis reaction a short substrate by RNase E by up to 50% in a mixed inhibition pattern. Inhibition of the decay of the long RNA substrates RNA1 or *dsbC* was much more severe with the RNA processing activity becoming reduced by as much as 80%. These studies have delineated the kinetic consequences of inhibition by RraA and RraB and provide further insights into the mechanisms that control RNA decay in bacteria.

Table of Contents

LIST OF TABLES

LIST OF FIGURES

CHAPTER 1 RESEARCH BACKGROUND

Overview

The cleavage of RNA by ribonucleases is a fundamental process for cell survival and for adaptation to different environments. RNase E is an essential endonuclease that plays a key role in RNA turnover and is conserved amongst proteobacteria. RNase E homologues have also been identified in Achaea and plants. RNase E is the central component of a multi-enzyme complex known as the RNA degradosome, which is involved in both the general degradation of mRNA and in posttranscriptional gene regulation.

The degradosome is a 500-700KDa complex formed by the assembly of the enzymes polynucleotide phosphorylase (PNPase), the DEAD-box family helicase RhlB, and the glycolytic enzyme enolase onto the C-terminal half of the RNase E protein. Besides those major components, other proteins are found associated with the degradosome under certain conditions, such as the chaperone DnaK and the DEAD helicase RhlE and CdsA. Whether degradosome formation is required in mRNA decay *in vivo* has been controversial. It is known that the majority of enolase and Pnpase are unattached to RNase E *in vivo*. Furthermore, RhlB and Pnpase can form a protein complex independent of RNase E.(Bernstein, Lin, Cohen, & Lin-Chao, 2004) While the overall significance of the degradosome has been established, how the individual component enzyme cooperate in carrying out RNA degradation or how changes in the degradosome composition affect the decay of different transcripts are still not clear. (Carpousis, Luisi, & McDowall, 2009)

RNase E protein structure and function

The *E.coli* RNase E protein which is encoded by *rne* gene, comprises 1061 residues and can be divided into three major functional portions: The N terminal portion contains the endoribonuclease activity domain and a zinc finger region; the central portion includes membrane anchoring segment A and its flanking regions, followed by Arginine rich RNA binding domain (ARRBD); the C terminal portion is a natively unstructured protein segment which binds to other major degradosome components. Structural and functional analysis of the N terminal portion and the co-crystallized of the C terminal fragments to its binding proteins have converged to the advanced understanding in function and regulation of RNA degradosome.

THE N TERMINAL HALF OF RNASE E

The N terminal (1 to 529 amino acids) of the RNase E catalytic core contains a large domain (1-400) which contains the substrate binding and the catalytic sites, a Zn-link region(401-411) which binds to Zinc ions and a small domain (415-529) which is involved in sub-domain organization. The crystal structure revealed that the RNase E holo enzyme comprises of four N terminal domain monomers (the rest of the protein is unstructured and hence cannot be detected by X-ray crystallography).

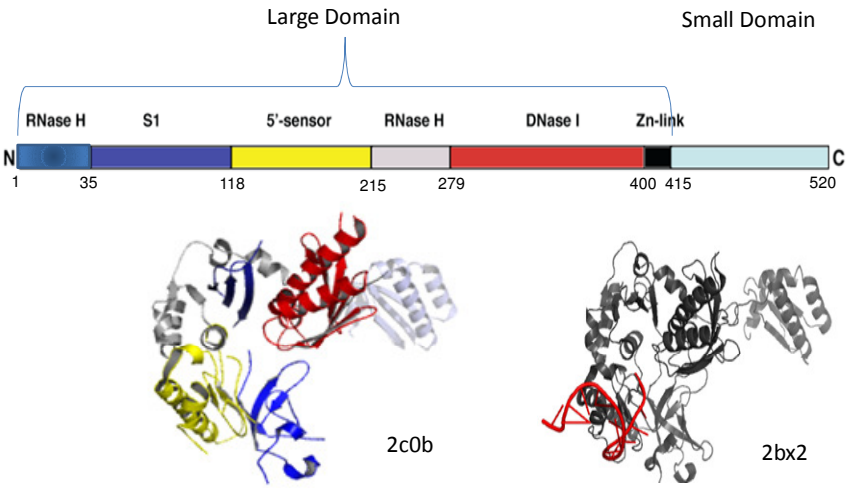

Figure 1.1 Crystal structure of N-terminal Catalytic Half of RNase E (Adapted from Callaghan et al., 2005a)

The large domain starts with two RNase H-like domains within which embedded a S1 RNA binding domain followed by a 5′ sensor region (Callaghan et al.2005b). RNase H is a non-specific endonuclease which cleaves the 3´-O-P bond of RNA in a DNA/RNA duplex, producing 3´-hydroxyl and 5´-phosphate terminated products. The RNase H like domains in RNase E functions structurally, *i.e.*it presents RNA substrate to the activity site, but there is no RNase H activity involved. Two of the well studied *rne* temperature sensitive mutants, *rne-1* (Gly 66 to Ser) and *rne-3071*(Leu 68 to Phe) which cannot grow at elevated temperatures presumably due to its inability to process rRNA and tRNAs have been mapped to the S1 RNA binding domain. Because RNA substrate binding involves both the S1 domain and the 5′ sensor, compensatory amino acids substitutions have been

found in the 5′ sensor region to suppress these temperature sensitive mutants. For example, *rne-187* (Arg187 to Leu) can suppress both *rne-1* and *rne-3071*. In these double mutants (*rne187/rne-1* and *rne187/rne3071*), the 5S rRNA processing and tRNA maturation is restored, however mRNA decay remains defective. This indicates that RNase E may utilize different strategies towards different RNA substrates (Perwez et al., 2008). In addition to RNA binding, the S1 domain also participates in the dimerization of RNase E catalytic core. Another dimer interaction is located within the conserved Cys motif which forms a zinc link between two protomers. These two interactions are referred as the isologous interface in the tetramer. (Callaghan et al., 2003)

RNase E has been demonstrated to prefer 5′ mono-phosphate RNA substrates, with 20-30 fold higher *in vitro* activity towards mono-phosphate RNAs than tri-phosphate RNAs when using 9S RNA or *rpsT* mRNA as substrates (Mackie, 1998). Recent work showed that 5′ mono-phosphate requirement for RNase E catalysis is dispensable *in vivo*. A mutation located in the 5′ sensor (R171Q), which shows disrupted RNA binding and significant reduced activity *in vitro*, is still viable albeit its slower growth rate and reduced tRNA processing ability in some cases (Garrey et al., 2009) Moreover, in contrast to previously studied tri-phosphate 9S RNA and tri-phosphate RNA1 which are stable because of their 5′ tri-phosphate protection, the tri-phosphate *cspA* mRNA, can be rapidly degraded by RNase E NTH regardless of its 5′ phosphate status. Notably the cleavage of 9S RNA and RNA1 by RNase E are different from that of the *cspA* mRNA. 9S RNA and RNA1 both contain an extended A/U rich 5′ single stranded region, where

RNase E has “direct” entry. However, the cleavage site of the *cspA* mRNA is relatively downstream, it is a short single stranded region bracketed by two step loop structures, significantly distant from the 5′ end, therefore requires “internal entry” of RNase E. (Kime, Jourdan, Stead, Hidalgo-Sastre, & McDowall, 2009). Although this phenomenon seems to be complex, the current understanding is that “direct” entry, compared to internal entry of RNase E, relies more on 5′ phosphate status (Jourdan, Kime, & McDowall, 2010). Therefore, RNase E substrate specificity involves more than just the 5′ sensor region, especially with long, structured RNA substrates. Other regions involved in substrate binding will be discussed in detail below.

The second half of the large domain is DNase I region that contains the active site. Based on the solved crystal structure of RNase E N terminal catalytic half protein (trapped with a 13mer allosteric RNA substrate), amino acids located in DNase I region, namely, Asp303, Asp346 and Asn305 are predicted to be the active site residues. These residues are in cooperation with a magnesium ion which is hydrated and is in proximity to RNA phosphate backbone (Callaghan et al., 2005b). In another effort to identify key amino acids in the catalytic domain of RNase E essential for function, several mutations within the DNase I domain that cause defects in RNA substrate binding but remain catalytically active have been identified (e.g. A326T and L385P) suggesting an additional role of DNase I region in RNA binding, especially for highly structured, natural RNase E substrates (Shin et al., 2008).

Between the large and small domains of N-terminal RNase E, there is a zinc link region (401-411aa). This region is conserved in the RNase E protein family among species, with each protomer contributing two cysteine thiols towards chelating the metal ion, *i.e.* two protomers share one zinc ion. Formation of the tetramer, or more precisely, dimer of dimers, requires both S1 domain dimerization (Schubert et al., 2004), Zn-link interactions (forming the isologous interface) and a domain-domain interaction between the small domains (heterologous interface). The heterologous interface between small domains is independent of the zinc-link and more flexible compared to the isologous interface. This flexibility is reflected in the "induced fit" during substrate binding. Upon binding to RNA substrate, the heterologous interface bends 60 degrees to bring RNase E to a relatively closed conformation (Koslover et al., 2008a).

THE C TERMINAL HALF OF RNASE E

The C terminal half of RNase E is less conserved and is unstructured. It consists of 4 segments of increased structural propensity (RISP), designated as segments A, B, C, and D. These segments interact with other cellular components, namely, the cytoplamic membrane, RNA, or with the other protein components of the degradosome (Callaghan et al., 2004).

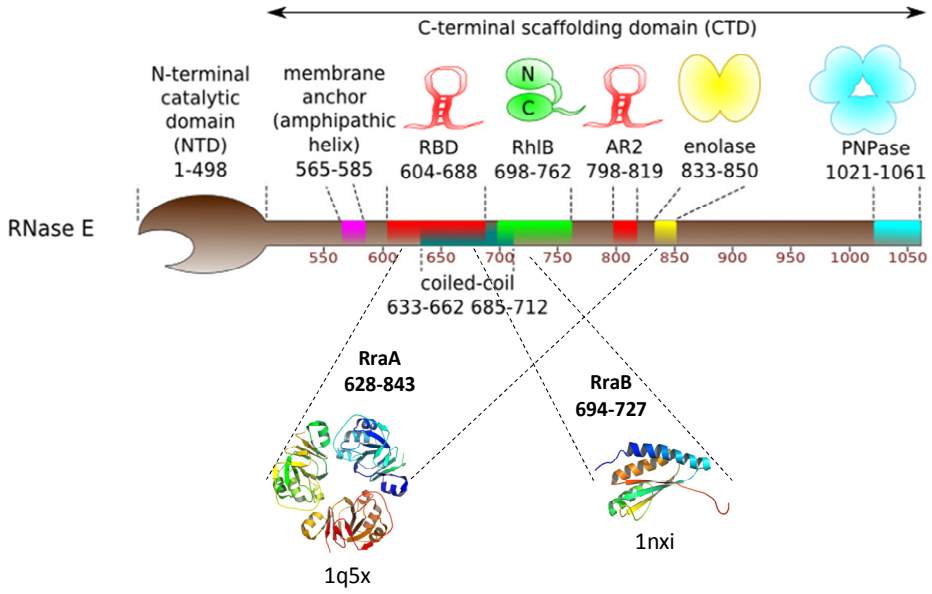

Figure 1.2 Schematic map of RNase E C terminal scaffolding domain. (Adapted from Gorna et al., 2010)

Previously, RNase E is known to form a cytoskeleton-like structure attached to cell membrane. It has been suspected that this organization is related to its interaction with cytoskeletal protein, namely the unique bacterial cytoskeletal protein MinD. Although RNase E is found to interact with MinD in a yeast two hybrid analysis, the cytoskeleton-like organization of RNase E is independent of MinD, or the other known cytoskeletal structure protein MreB which is the actin-homolog in bacteria (Taghbalout & Rothfield, 2007). This mystery was solved later by *in vitro* analysis: the membrane-anchoring domain of RNase E has been defined, which is Segment A (568-582aa). Segment A forms an amphipathic helix that can bind to lipid vesicles with the dissociation constants

at approximately 1μM. In agreement with this observation, the RNase E full length protein is also able to bind phosphor-lipid vesicles. In addition, interaction with phosphor-lipid vesicle does not affect the endoribonuclease activity of RNase E (Khemici, Poljak, Luisi, & Carpousis, 2008). However, RNase E mutant with deletions of segment A has a slower growth rate and smaller colony size compared to wild type. It is likely that cytoskeleton-like organization of RNase E plays important role in its cellular function. One promising hypothesis is that membrane-anchoring is a storage mode of RNase E which limits its cytoplasmic availability. This is in agreement of the excess amount of RNase E protein detected *in vivo* as discussed in RNase E transcription regulation part below. In this notion, the loss of membrane-anchoring could result in elevated RNase E activity which is toxic to normal growth.

As mentioned above, previous studies focused on the catalytic core of RNase E implied the existence of alternative RNA substrate binding sites. In the central region of RNase E, following the segment A, there is an Arginine Rich RNA Binding Domain (ARRBD, 604-688aa), which contains the first coiled coil structure (633-652aa) and partially overlaps with Segment B (633-712aa). Segment B contains two coiled coil structures, 633-652aa and 685-712aa. The Arginine Rich domain, along with the two coiled coil structures E have been shown to mediate the binding of substrate RNAs, even without the N terminal catalytic core of RNase E (Taraseviciene, Laimute, Bjork, Glenn R. And Uhlin, 1995). Segment B also overlaps with the RhlB interaction site. The region of RNase E which interacts with RhlB was first referred to as the R region (628-843aa),

(Callaghan et al., 2004) and then refined to a smaller fraction within the R region (698-762aa) (Chandran et al., 2007a). Both of these fragments can stimulate the ATP dependent RNA unwinding activity of RhlB, with 628-843 fragments being comparably more efficient than the 698-762 fragments. It is quite common in DEAD box helicases that RNA binding is enhanced upon binding of the helicase to other proteins. In the case of RhlB, the RNA binding affinity which is mainly located in the C terminal region of protein is enhanced cooperatively in the presence of RNase E 628-843aa fragment. Indeed, the 628-843aa fragments contain a second RNA binding region (AR2), which is also Arginine rich (798-819aa). Both RNA binding domains in the central region (628-843aa) could contribute to the enhanced binding of substrate in RNase E (628-843aa)/RhlB complex compared to RhlB alone (Chandran et al., 2007a). The cooperation between RhlB and RNase E is substrate specific. It is possible that such cooperative action is only required for highly structured complex RNA substrate, such as RNA1, yet not necessary for RNA substrates that can be processed by cellular nucleases other than RNase E (Nishio & Itoh, 2009).

Segment C (839-850aa) of the RNase E C terminal scaffold domain is conserved among a subgroup of -bacteria and serves as the binding site for enolase. The RNase E CTD-enolase complex does not bind to Pnpase, because it excludes the segment D, which binds to Pnpase. It is noteworthy that the native RNase E CTD-enolase complex does not bind to RhlB even through it contains an RhlB binding site (Callaghan et al., 2004) Binding of RNase E fragments does not change enolase activity. Moreover, only one

tenth of the enolase inside the cell is sequestered into the degradosome complex. In fact the function of enolase in degradosome is still unclear. One interesting hypothesis is that enolase relates cellular energy level to post-transcriptional gene regulations (Callaghan et al., 2004).

The aforementioned Segment D (1021-1061aa) of RNase E binds to the periphery region of Pnpase in a pseudo-continuous anti-parallel beta sheet fashion. Similar to enolase, this interaction does not affect Pnpase activity, probably due to its distance from the active site of Pnpase. The stoichiometric ratio between monomers of RNase E and Pnpase is 1:1. The binding affinity between the 20 amino acids RNase E C terminal fragment and Pnpase trimers is about 0.9 μM as measured by ITC. Because RNase E is a tetramer *in vivo*, the affinity between full length RNase E and Pnpase could be much lower than 0.9 μM (Nurmohamed, Vaidialingam, Callaghan, & Luisi, 2009a).

Regulation of RNase E

TRANSCRIPTIONAL REGULATION OF RNASE E

Regulation of RNase E is crucial to cell survival given its essential role in processing rRNAs and decay of mRNA. *Rne* is transcribed from three promoters, *p1, p2* and *p3*. *rne* transcribed from any of these promoters on a single copy vector can support cell growth of an *rne1018::bla* deletion mutant(Maria C. Ow, Qi Liu, Bijoy K. Mohanty & Andrew, 2002) Measuring *rne* transcript levels and RNase E protein in mutants utilizing either the *p1, p2* or *p3* promoter only led to some intriguing findings: transcription from

either one of the two weak promoters (*p2 and p3*) resulted in low steady levels of *rne* transcript, but auto regulation (see below) was lost and therefore the transcript had a half-life. However the RNase E protein level expressed from the weak promoter was reduced more than 10 fold compared to wild types. Moreover, cells with less than 20% of "normal" level of RNase E protein appeared to function properly in terms of mRNA decay, implying that under "normal" conditions, RNase E may be present in large excess.

POST-TRANSCRIPTIONAL REGULATION OF RNASE E

Extensive bioinformatics and genetics analyses have delineated the post-transcriptional control of *rne* mRNA. RNase E auto regulates its translation and hence its cellular activity by modulating the *rne* mRNA degradation rate. (Jain & Belasco, 1995) This auto regulation is achieved in *cis via* the first 361 nucleotides in the *rne* 5′ UTR. Despite the sequence divergence, the secondary structure of RNA in this region is well conserved among different bacteria species. This 361nt region can be further dissected into 3 hairpin (hp) loops and 3 single stranded regions located in between the hairpin loops. Deletion and substitution analysis revealed that hp2 and hp3 are core elements that mediate *rne* auto-regulation (Diwa, Bricker, Jain, & Belasco, 2000). Specifically, the 8 nucleotides internal loop located near the top of hp2 is essential for this regulation (Diwa & Belasco, 2002). The role of hp2 was further elucidated in a recent study that showed that it binds to the N-terminal catalytic core of RNase E forming two different complexes (productive and unproductive). The productive complex facilitates cleavage elsewhere in the transcript. Three alanine mutations in RNase E (F57, R169 and N323) severely impair

hp2 binding. These mutations are located at the S1 RNA binding domain, 5′ sensor region and the DNase I region. However, one of the earliest studies on RNase E regulation claimed that auto-regulation is compromised when the central region (591-601aa) of RNase E is deleted, as demonstrated by the level of β- galactosidase activity from an *rne-lacZ* transcriptional fusion, suggesting that alternative interaction sites may exist (Jain & Belasco, 1995). The importance of RNase E C-terminal half for its autoregulation was further illustrated by studies using the *rneΔ*610 mutant, which contains only the N-terminal catalytic half of RNase E (i.e. 610 residues were deleted from the C-terminal). In this mutant, the processing of *rne* transcript is impaired. Specifically, the mutant very poorly cleaves within the *rne* 5′ UTR with only approximately one eighth of the wildtype cleavage efficiency is observed (Ow, Liu, & Kushner, 2000).

POST-TRANSLATIONAL REGULATION OF RNASE E

Another level of RNase E regulation occurs after translation. To date, three small proteins have been identified to modulate RNase E activity by binding to RNase E C-terminal region: RraA, RraB and the L4 ribosomal protein (Gao et al., 2006; Lee et al., 2003; Singh et al., 2009). These small proteins regulate the cleavage of a subset of transcripts by mechanisms that are not fully understood.

The Components of the RNA degradosome

RHLB

E. coli has five DEAD box proteins, which further belong to the DEXD/H protein family. DEXD/H proteins are mostly involved in DNA and RNA metabolism. The five DEAD box proteins are RhlB, RhlE, SrmB, CsdA and DbpA. Sequence alignments of these five proteins shows that: they share a common DEAD-box core (about 350aa), with various short N-terminal extensions (2-9aa) and different C-terminal extensions (70-290 aa). The short N-terminals have no known roles, whereas the extended C-terminals are thought to interact with other proteins and RNAs.

Most of the DEAD box proteins in yeast are essential however, the DEAD box proteins in *E.coli* are not essential under common laboratory growth conditions. Even various combinations of double knockout mutants can grow, although *csdA* mutants display cold sensitivity. SrmB, CsdA and DpbA are involved in ribosome biogenesis whereas RhlB and CsdA participate in mRNA degradation. The role of RhlE remains unknown.

As noted before, the RhlB protein contains an N-terminal DEAD box core which contains seven key conserved motifs (I, Ia, Ib, II, III, Q and GG), the C-terminal (267-421aa) domain which contains four motifs (IV, V, VI and QxxR) and an arginine-rich basic tail (398-421aa) (Iost & Dreyfus, 2006).

The DEAD box proteins have two biochemical activities *in vitro*: RNA-dependent ATPase activity and ATP–dependent RNA helicase activity. The RNA-dependent

ATPase activity is believed to occur in a cycle in which ATP-bound protein binds RNA, followed by the conversion from ATP to ADP and subsequent release of RNA. Exogenous RNA is required for ATPase activity. The assay can be continuously monitored by the release of phosphate (Chandran et al., 2007a) or by coupling ATP hydrolysis to NADH oxidation (Cartier, Lorieux, Allemand, Dreyfus, & Bizebard, 2010). DEAD box proteins unwind only a few base pairs during each ATP hydrolysis cycle. Unlike non-DEAD box helicases, DEAD box helicases have very poor processivity because they cannot prevent the unwound region to re-anneal. Hence, DEAD box helicases can only unwind RNA helices within 10 base pairs or less, which corresponds to an energy barrier of approximately 20kcal/mol. (Iost & Dreyfus, 2006). The unwinding activity can be assayed by measuring the conversion of duplex RNA to monomers which are separated by electrophoresis. A continuous helicase assay has been developed recently by Cartier *et al.* using complementary oligonucleotides that are labeled with Cy5 or Cy3 fluorophores at the 3′ or 5′ extremities (Cartier, Lorieux, Allemand, Dreyfus, & Bizebard, 2010).

In contrast to the other four DEAD box proteins, RhlB does not have detectable activity on its own. Both the ATPase and helicase activity of RhlB are stimulated by binding to the RNase E protein fragment (628-843aa). As noted above, the interaction site of RhlB is situated at the C-terminal extension region of RNase E. However the Arginine-rich basic tail is not required for this interaction. The binding affinity between RhlB and RNase E (628-843) is in the 50nM range with a stoichiometric ratio of 1:1. The

interaction of RNase E and RhlB boost the RhlB ATPase activity by at least an order of magnitude. Saturating amounts of RNase E (628-843) fragment are able to increase RhlB unwinding activity by more than 5 fold (Chandran et al., 2007a). There is an important caveat that applies to this assay. The experiment was done under conditions that RNA substrate is much less than enzyme (1:100 folds or less) in order for the unwinding reaction to happen irreversibly, due to the poor processivity of helicases discussed above.

ENOLASE

Enolase is a glycolytic enzyme catalyzing the reversible dehydration of 2-phosphoglycerate to phosphoenolpyruvate. It is a universally conserved enzyme found in all three domains of life. In *E. coli*, enolase is a 48 kDa protein composed of two domains. The N terminal domain (1-142aa) consists of three anti-parallel β sheets followed by four α-helices. Interestingly, the helical domain of Pnpase from *S. antibioticus* shares structural similarity with the first three α-helices in the N-terminal domain of enolase. This observation raises the possibility that the *E. coli* enolase can bind RNA. The enolase C-terminal principal domain (143-431aa) is an 8-fold TIM barrel structure albeit with an unusual topological organization. The active site is at the C-terminal ends of the β strands of the barrel. The *E. coli* enolase is a dimer which requires two magnesium ions per subunit to function. In yeast, enolase binds DNA or RNA and this binding inhibits its catalytic activity. Whether this is true in *E.coli* waits testing (Kühnel & Luisi, 2001).

It should be stressed that only one tenth of the enolase in the cytoplasm is recruited to the RNA degradosome. Enolase binds to the unstructured region of RNase E C terminal domain described above. The segment C peptide inserts into the dimer interface. The RNase E interaction region on enolase is remote from its active site as demonstrated by the co-crystallized enolase and segment C structure (Chandran & Luisi, 2006), which is consistent with the previous finding that binding with RNase E does not affect enolase catalytic activity. The function of enolase in RNA degradosome is unclear. It has been proposed that enolase interaction with RNase E serves as a mediator to link the cellular energetic state with post-transcriptional regulation. As mentioned above, the RNase E CTD-enolase complex does not bind to RhlB even through it contains the RhlB binding site(Callaghan et al., 2004), which suggests that enolase might play a structural role in the RNA degradosome.

PNPASE

Pnpase is a dual-function enzyme that catalyzes a reversible reaction: as a phosphorylase it degrades RNA in the 3′ to 5′ direction to produce nucleotide diphosphates (NDPs); as a polynucleotide synthase it adds tails to 3′ end of RNA in a template-independent manner. Besides this reverse reaction, Pnpase also catalyze the exchange of the β-phosphate group of nucleoside diphosphate and free orthophosphate. Because phosphorylysis is a near equilibrium reaction, the direction of the reaction is largely dependent on the availability of phosphate: high concentration of phosphate favors the degradation whereas excess

amount of diphosphates and low phosphate concentration promotes the 3′ terminal oligonucleotide polymerase activity.

Mutants devoid of Pnpase grow normally at typical laboratory culturing conditions, but display impaired growth at lower temperatures. In RNase II or RNase R mutants, Pnpase is indispensable. Moreover, a recent study showed that Pnpase is responsible for degradation of oxidized RNAs and thus relieves cells from oxidative challenges (Wu et al., 2009).

Pnpase exists in all three primary kingdoms. The *E.coli* Pnpase is a homotrimer consisting of 78 kDa subunits. Each subunit is composed of five domains: the N-terminal contains two homologous RNase PH domains which serve as the structural core, linked by an all α-helix domain at the bottom; on top of this core structure sit two C-terminal RNA binding domains, KH and S1. The core RNase PH where the active site is situated at is conserved, as is the overall donut ring structure that forms a central channel for catalysis. Interestingly, in eukaryotes the ring structure is conserved in the yeast and human exosome, however the exonucleolytic activity is hydrolytic rather than the phosphorolytic activity found in prokaryotes. It appears that the active site residues are located at the RNase PH core. Metals ion (magnesium or manganese) is required for activity; the all α-helical domain is also implicated in catalysis. Truncation mutants without the C terminal KH or S1 RNA binding domains still catalyze phosphorylysis, with a significant increase in K_m and more importantly, lack of processivity.

In *E. coli*, Pnpase can be found in two complexes: the RNA degradosome where it binds to RNase E C terminal (segment D), or in the Pnpase-RhlB complex. The interaction site with RNase E is located at the periphery of the core ring structure, with affinity to the segment D peptide in the micromolar range and a stoichiometric ratio of 1 (protomer). It is noteworthy that the KH and S1 domain at the C terminal of Pnpase do not affect this interaction. In comparison, the binding between Pnpase and RhlB are much stronger (0.9μM for RNase E binding vs. less than 25nM for RhlB binding). Moreover, the interaction is independent of the RNase E C-terminal region (Liou, Chang, Lin, & Lin-Chao, 2002). RhlB also shows functional interactions with Pnpase independent of RNase E. It unwinds duplex RNA for Pnpase to carry out phosphorylysis. Of particular relevance to this interaction, Pnpase requires 7-9 bases of single-stranded RNA at the 3′ end for binding (Carpousis, Luisi, & McDowall, 2009).

The regulation of Pnpase is complex. There is a stable double stranded RNA structure in the 5′ UTR of the *pnp* mRNA, which prevents its processing. Following the disruption of the double strand structure by RNase III, the newly generated 3′ end is subject to Pnpase degradation. Once the stem in the 5′ UTR is destroyed, the *pnp* mRNA becomes sensitive to RNase E. An earlier model proposed that Pnpase binding to the 5′ UTR stem structure prevents translation thus making the mRNA vulnerable to degradation. However, recent work by Carzaniga *et al.* argued that translation is involved in Pnpase auto regulation. The role of Pnpase in its auto regulation is that, after RNase III step, it transforms a stable

RNA with 5′ stem structure into a 5′ single stranded RNA which is further degraded by RNase E in a Pnpase-independent manner (Carzaniga et al., 2009).

As mentioned above, the level of NDP and phosphate determines the direction of the Pnpase reaction. It also has been proposed that adding nucleotides onto the 3′ tail of RNA can facilitate the phosphorylysis reaction given that Pnpse need a 3′ single strand "handle" no shorter than 7 bases long. Another layer of complexity in Pnpase regulation comes from the role of ATP. It has been reported that ATP at concentration of 5mM or higher inhibits Pnpase activity in both directions. Pnpase-dependent tailing or degradation of RNA mainly occurs at low energy charge. When the ATP concentration is high, other enzymes may play more significant roles in RNA processing. In that regard, in the Pnpase-RhlB complex or the RNA degradosome, RhlB as an ATP-dependent RNA helicase converts ATP to ADP as it unwinds RNA duplex, decreases the "local" ATP concentration of its proximate Pnpase and helps relievethis inhibition (Del Favero et al., 2008).

RraA, RraB and other Minor components in RNA degradosome

Following its discovery about 16 years ago, the *E. coli* RNA degradosome has been characterized by many groups around the world. Besides the major components in the complex, several minor components have been found in sub-stoichiometric amount such as CsdA, PPK, GroEL, DnaK and Hfq. During bacterial adaptation to cold temperatures, the RhlB helicase is partly substituted with the cold shock helicase, CsdA thereby forming a "cold shock degradosome". The mechanism underlying this degradosome

remodeling awaits more investigation. Likewise, a polyphosphate kinase (PPK) has also been co-purified in the degradosome complex, but the physiological significance of this enzyme is not known. GroEL and DnaK are chaperone proteins which may be recruited to assist proper protein folding of RNase E. The RNA binding protein Hfq is implicated in many small RNA regulation processes. Since no direct protein-protein interactions were detected with highly purified Hfq, the current understanding is that Hfq is recruited to the degradosome complex via mediating RNA. Hfq binding to small RNAs initially protects them from degradation and mediates their interaction with target mRNA in the translation initiation site. Upon repression of translation, both sRNA and mRNA are degraded by RNase E. In this respect, the recruitment of Hfq to the degradosome promotes cleavage of RNA that binds to Hfq (Worrall et al., 2008).

Two protein inhibitors of RNase E, RraA and RraB (regulators of ribonuclease activity A and B) have been discovered by our group using genetic screens (Lee et al., 2003). *In vivo* studies demonstrated that these inhibitors can bind to the C-terminal domain of RNase E and remodel the structure of degradosome complex, consequentially affecting a large group of *E. coli* transcripts (Gao et al., 2006). Homologs of RraA exist in bacteria, Achaea and plants, whereas RraB homologs are found only in γ-proteobacteria. Of particular relevance to the current study, RraA and RraB both can inhibit the activity of RNase ES, a functional ortholog of RNase E from *Streptomyces coelicolor.* (Yeom et al., 2008) Moreover, RraAV1, a homolog of *E.coli* RraA from *Vibrio vulnificus* that shares 80% identity can effectively inhibit *E.coli* RNase E activity (Lee, Yeom, Sim, Ahn, &

Lee, 2009a). It is noteworthy that another inhibitor of RNase E, the ribosomal protein L4 interacts with the degradosome to affect a set of 85 transcripts that are related to stress response (Singh et al., 2009).

Microarray studies revealed drastic changes in the transcriptome of cells which over-express RraA/RraB: 336 transcripts were stabilized by either RraA or RraB, 371 transcripts were affected uniquely by the over-expression of RraA whereas 85 transcripts were stabilized only by RraB.

Research Outline

The discovery of RraA and RraB revealed a new mechanism for the global regulation of mRNA abundance. This work has raised several questions: First, why do such small inhibitory proteins exist in the genome? What is the physiological significance of these genes? Second, how does the binding of RraA or RraB affects the detailed kinetics of RNA hydrolysis by RNase E or in concert with other degradosome components? I have combined genetics and biochemistry methods to address these questions.

In chapter 2, I describe the transcriptional regulation of *rraA* and *rraB*. In Chapter 3, I describe the reconstitution of the RNA degradosome by individually purified major components. The interactions between those components were demonstrated by immunoprecipitation. In chapter 4, the inhibition RNase E-mediated hydrolysis of short and long, structured RNA substrates by RraA or RraB is detailed. The degradation of long, structured RNAs is shown to require a coordinated action of different degradosome

components. In the appendix, I have included preliminary results from proteomic experiments regarding how remodeling of RNA degradosome affect global protein abundance.

CHAPTER 2 TRANSCRIPTIONAL REGULATION OF RRAA AND RRAB.

Introduction

RraA (regulator of ribonuclease activity A), is an evolutionarily conserved 17.4-kDa protein with close homologs (>40% amino acid identity) in bacteria, Achaea, proteobacteria, and plants. RraA binds to RNase E with an equilibrium dissociation constant (K_D) in the nano molar range and serves as a trans-acting modulator of the endonuclease activity of the enzyme (Gorna et al., 2010). High-affinity binding requires the C-terminal half region of RNase E, which acts as a scaffold for the assembly of a large multi protein complex called the degradosome (Gao et al., 2006; Gorna et al., 2010; Vanzo et al., 1998). RraA appears to interact with RNase E and RhlB and by doing so masks the enzyme′s binding site for RNA substrates (Gorna et al., 2010). Gene chip analysis revealed that the action of RraA results in a dramatic change in the global abundance of mRNAs in *E.coli*, affecting over 15% of all cellular transcripts. Importantly, the gene expression profile that is obtained upon over expression of RraA is distinct from that obtained upon depletion of RNase E or through the action of RraB, a second trans-acting RNase E inhibitor of *E. coli* (Gao et al., 2006). The *rraA* gene is located downstream of *menA*, which encodes a 1, 4-dihydroxy-2-naphthoic acid octaprenyltransferase that catalyzes the prenylation of the redox mediator menaquinone (Shineberg & Young, 1976). Transcription of *menA* appears to occur from a σ^{70}-dependent promoter. Earlier, Meganathan proposed that *rraA* (formerly designated *menG*) is transcribed from the *menA* promoter in a dicistronic mRNA (Meganathan,

1996). However we demonstrated that *rraA* is transcribed predominantly from its own promoter (P_{rraA}) located in the intergenic regions between *menA* and *rraA* genes. Transcription from P_{rraA} is σ^S-dependent and is induced upon entry into stationary phase. Furthermore, we showed that the synthesis of RraA is regulated at the post-transcriptional level by RNase E, suggesting the existence of a feedback regulatory circuit whereby induction of *rraA* transcription occurs in a σ^S-dependent manner and results in inhibition of RNase E activity, in turn decreasing the degradation rate of the *rraA* transcript (Zhao, Zhou, Kawarasaki, & Georgiou, 2006).

RraB, previously annotated as YjgD in the NCBI database, is a 15.6 kDa protein that interacts with RNase E and inhibits RNase E endonucleolytic cleavages in *E. coli*. In contrast to RraA which has homologues in numerous bacterial genomes, RraB is only found in γ-proteobacteria, suggesting that the latter protein may have a more specialized role in modulating RNA degradation. Similar to RraA, RraB does not alter RNase E cleavage site specificity nor does it interact detectably with the substrate RNAs. RraB also possesses similar affinity for RNase E as RraA. However, RraB exhibits key differences in its mode of action and its effects on the transcript profile. RraB interacts with residues 694-727 at the C terminal half of RNase E (Gao et al., 2006). Over expression of RraB from a high copy plasmid induces specific changes in degradosome composition that are distinct from those mediated by RraA over expression. Importantly, the action of RraB results in a dramatic change in the global abundance of mRNAs that is different from that obtained through the action of RraA (Gao et al., 2006). The existence

of two cellular proteins that exert differential effects on RNA decay via their interactions with RNase E and degradosome remodeling argues that modulation of RNA stability may be a mechanism for global control of transcript abundance in response to dynamic changes in the environment.

The *E. coli rraB* gene is 417 bp in length and is located at 96.4 minutes on the chromosome, adjacent to *argI* which is transcribed from the opposite strand and codes for ornithine carbamoyltransferase I. Here we show that *rraB* is transcribed from its own promoter (P_{rraB}) which is divergent from the *argI* promoter and overlaps with the arginine repressor binding site (ARG box) (Makarova, Mironov, & Gelfand, 2001) located in the *argI-rraB* intergenic region. However we found no evidence that the promoter of *rraB* is regulated by the transcription factor ArgR or the availability of arginine. A screen for transposon insertions that enhance the β-galactosidase activity from a Φ(P_{rraB}-*lacZ*) transcriptional fusion led to the isolation of a *glmS852::Tn5* allele that upregulated *rraB* transcription by about 5-fold. The *glmS852::Tn5* allele resulted in a decrease in the cellular UDP-GlcNAc level to less than 50% of the level observed in the parental strain. Furthermore, β-galactosidase activity from an *rne-lacZ* fusion increases in the *glmS852::Tn5* mutant. Since the *rne-lacZ* transcript is a substrate of RNase E, the increase in β-galactosidase activity indicates that the *rne-lacZ* fusion is stabilized as a result of a reduction in RNase E activity, presumably a consequence of enhanced inhibition by the increased expression of RraB.

Materials and Methods

STRAINS AND PLASMIDS

The strains, plasmids, and phage vectors used in this study are listed in Table 2.1. The plasmid pBAD30-glmS was constructed as follows: the glmS gene coding sequence was amplified by PCR from genomic DNA of strain MC4100 using the following primers: glmS5 (5′-CGGCGGGGTACCAGGAGGTTACGATGTGTGGAATTGTTGG C-3′) and glmS3 (5′-CGGCCCAAGCTTTTACTCAACCGTAACCGATTTTGCCAGG TT-3′). The PCR product was digested with KpnI and HindIII and then ligated into the plasmid pBAD30 that was similarly digested.

Table 2.1 Strains, plasmids and phage vectors

Strains, plasmids, and phage vectors	Description	Reference or Source
BW21116	*Δlac-169, creC510, hsdR514, uidA(ΔMluI)::pir+*	(Haldimann, Daniels, & Wanner, 1998)
CAG51025	MC1061 *φλ[rpoH P3::lacZ] ΔrseB nadB-3140::Tn10, ΔdegS arg::Tn5,*	(Haldimann, Daniels, & Wanner, 1998)
CJ1825	MC1061 (*λez1*)	(Gao et al., 2006)
DHB4	*(ara-leu)7697 araD139 _lacX74 galE galK rpsL phoR (phoA)PvuII malF3 thi/F lac-pro lacIq*	(Denisot, Le Goffic, & Badet, 1991)
EC-O	*thi-1, relA1, Δ(pro-lac)X113[del = DE5] supE44 / F42-114(FTs) lac*	(Simons, Houman, & Kleckner, 1987)
JCB570	MC1000, *phoR zih12::Tn10*	(Bardwell, McGovern, & Beckwith, 1991)
JCB571	MC1000 *phoR zih12::Tn10 dsbA::kan*	(Bessette, Qiu, Bardwell, Swartz,

		& Georgiou, 2001)
KS474	*F-lacX74 galE galK thi rpsL(strR) ΔphoA(Pvull) degP41(ΔPstl)::Ω kanR*	(Strauch, 1988)
LZ001	{P90C, λ (-152 to -1 nt)-*lacZ* }	This study
LZ002	{P90C, λ (-152 to -1 nt)-*lacZ*, *glmS852::Tn5* }	This study
LZ003	{CJ1825, *glmS852::Tn5*}	This study
MC4100	F-, *araD139, Δ (argF-lac) U169, flbB(flhD)5301, deoC1, ptsF(fruA)25, relA1, rbsR22, rpsL150, thiA*)	(Baker, Mackman, Jackson, & Holland, 1987)
Mjf256.10	{DHB4, *gshA::KmR _trxB::CmR ahpC (V164G)*}	(Faulkner, Veeravalli, Gon, Georgiou, & Beckwith, 2008)
MZB001	{EC-O, λ p0-*lacZ* }	This study
MZB002	{EC-O, λ (-239 to -1 nt)-*lacZ* }	This study
MZB003	{EC-O, λ (-152 to -1 nt)-*lacZ* }	This study
MZB004	{EC-O, λ (-239 to -153 nt)-*lacZ* }	This study
P90C	[ara Δ(lac-pro) thi]	(Miller, 1972)
pBAD30	pACYA184 ori, Amp^r, pBAD	(Guzman, Belin, Carson, & Beckwith, 1995)
pBAD30-glmS	pACYA184 ori, Amp^r , *glmS* under pBAD promotor	This study
pSP417	pBR322 ori, Amp^r MCS sites (8 restriction sites) upstream of a promoter-less lacZ	(Podkovyrov & Larson, 1995)
pMZB002	{pSP417, (-239 to -1 nt)-*lacZ* }	This study
pMZB003	{pSP417, (-152 to -1 nt)-*lacZ* }	This study
pMZB004	{pSP417, (-239 to -153 nt)-*lacZ* }	This study
λRS 45	bla′-lacZsc *imm21 ind* +	(Simons, Houman, & Kleckner, 1987)
λRS74	placUV5-lacZ *imm21 ind* +	(Simons, Houman, & Kleckner, 1987)
λMZB1	Same as λRS74, but containing the p0-*lacZ* fusion	This study
λMZB3	Same as λRS45, but containing the (-152 to -1 nt)-*lacZ* fusion	This study

GROWTH CONDITIONS

Unless otherwise stated, cells were grown in Luria-Bertani broth (LB) under aeration at 37°C, and growth was monitored by measuring the turbidity at 600 nm (A_{600}). Minimal media contained M9 salts (BD, SPARKS, MD), 50 μg/ml thiamine, 30 μg/ml proline, and 0.2% glucose or 20μg/ml glucosamine-6-phosphate (GlcN-6-P) or 0.2% glycerol. Media were supplemented with antibiotics, as required (50 μg/ml ampicilin, 25 μg/ml kanamycin or 10 μg/ml chloramphenicol).

RNA METHODS

For reverse transcriptase-polymerase chain reaction (RT-PCR) analysis, total RNA was isolated with the RNeasy kit (Qiagen, Valencia, CA) and treated with RNase-free DNase (Ambion, Austin, TX). 50 ng of total RNA was subjected to RT-PCR analysis using the One Step RNA PCR kit (TaKaRa, New York, NY). Northern blots were performed using total RNA isolated from *E. coli* JCB570 grown in LB medium under aeration at 37°C. Samples were collected in one hour intervals throughout the exponential and stationary phases. 5 μg of total RNA per lane was loaded onto a denaturing gel containing formaldehyde, and then transferred to a positively charged nylon membrane (Hybond N+, Amersham, UK). The AlkPhos direct nucleic acid labeling and detection system (Amersham, UK) was used to synthesize the oligonucleotide probe specific to *rraB* gene (5′-AACAACCTGATGACGCATGGCA-3′). Hybridization, washing of the membranes, and detection of signals were carried out according to the manufacturer′s instructions.

PRIMER EXTENSION

For primer extension, a 5′ ^{32}P-labeled primer (5′CACCACTGACATTGCCTCCACCTTT -3′) was used in the RT reaction with 5 g of total RNA (purified using RNeasy Kit, as described above) and SuperScript III RNase H- Reverse Transcriptase (Invitrogen, Carlsbad, CA). The primer extension products were separated on 6% polyacrylamide/7 M urea gels. The dideoxy-DNA sequence ladder from the same primer was prepared using the *fmol* DNA Cycle Sequencing System (Promega, Madison, WI).

REAL-TIME RT PCR

Cells were grown in M9 minimal media with 0.2% glucose and collected at A_{600}=0.2. Total RNA was isolated with the RNeasy kit (Qiagen, Valencia, CA) and treated with RNase-free DNase (Ambion, Austin, TX). Reverse transcription of 0.2 µg of total RNA was performed with random hexanucleotides and SuperScript III RNase H- Reverse Transcriptase (Invitrogen, Carlsbad, CA). The RT PCR was performed using primers (5′-TCGTGATTTGCTGCGACATC-3′) and (5′-ACCTGGGCATCGATCAGATC-3′) for rraB gene in the experiment. Primers (5′-TCGAACAGGTGGCGTTAAATG-3′) and (5′-GGAGCGCAAATGCAGACAT-3′) were used for dnaX gene as a control. Real-time PCR reactions were performed using ABI Prism 7900 (Applied Biosystems) under universal cycling conditions (2 min at 50°C, 10 min at 95°C, 40 cycles of 15 s at 95°C, and 1 min at 60°C). The reaction mixture (20 µl) contained 2× SYBR Green PCR Master Mix (PE Applied Biosystems), 10 pmol of forward and reverse primers, and 5 l of cDNA (0.1-10 ng). Sequence-specific standard curves were generated by using serial dilutions of cDNA and the quantity of rraB cDNA was normalized relative to dnaX

cDNA in each sample. Cycle threshold (C_T) values were determined by automated threshold analysis with ABI Prism version 2.3 software. Each experiment was performed at least three times with two independent RNA preparations.

LACZ FUSIONS

PCR amplification was used to generate DNA fragments between -239 to -1 nt in *rraB*. These fragment were cloned upstream of the lacZ gene in the multicopy transcriptional fusion vector, pSP417. The lacZ fusions were transferred into λRS45, and the negative control in pSP417 was transferred into λRS74 via double recombination(Simons, Houman, & Kleckner, 1987). Blue plaques containing the recombinant lambda phages were isolated and used to lysogenize strain EC-O (*Δlac*) to generate strains MZB001 to MZB004. All lysogens were tested for mono-lysogenization by PCR. A similar approach was employed for the transfer of the Φ (-152 to -1 nt) *rraB-lacZ* fusion into the strain P90C (*Δlac*) to generate LZ001.

To measure β-galactosidase activity, cultures were grown with aeration at 37°C in M9 medium overnight and subcultured into the fresh medium. To detect the effect of tryptophan or arginine limitation, cultures were grown in the appropriate media as described in supplementary material. Aliquots were collected, centrifuged at 4°C and re -suspended in an appropriate volume of ice-cold Z buffer (60 mM Na2HPO4, 40 mM NaH2PO4, 10 mM KCl, 1 mM MgSO4; pH 7.0) (Miller, 1972) to give OD600 in the range from 0.6 to 0.9. β-galactosidase activities were determined from at least three independent experiments (Miller, 1992).

TRANSPOSON MUTAGENESIS

50 ng of transposome (EZ-Tn5TM, Epicentre, Madison, WI) was electroporated into 50 µl (10^8 cells) competent cells of *E.coli* LZ001 strain. Transformed cells were grown on LB plates containing 25 µg/ml kanamycin and 25 µg/ml X-gal and incubated at 37°C overnight. Out of about 32,000 colonies that were screened, 6 showed an intense blue color consistently. Of these, one strain gave markedly higher β-galactosidase activity in liquid cultures. Genomic DNA from this clone was extracted using DNeasy kit (Qiagen, Valencia, CA), fragmented by EcoRI digestion and self-ligated using T4 DNA ligase (Roche, Switzerland). The ligation product was transformed into the *E. coli pir*$^+$ strain BW21116 (Haldimann, Daniels, & Wanner, 1998) and kanamycin resistant colonies were selected. Those colonies contained plasmids formed by circularized ligation products, made from partially digested genomic DNA containing the *R6Kγori* and kanamycin resistance cassette. Plasmid DNA was purified and sequenced using the primers R6KAN-2 and KAN-2 FP-1 provided by the EZ-Tn5^{TM} Kit.

DETERMINATION OF UDP-GLCNAC CONCENTRATION

The UDP-GlcNAc concentration in strains LZ001 and LZ002 was determined by HPLC. Cultures were grown in M9 minimal media to an A_{600} of 0.2 to 0.3 and the cell pellets were collected and deproteinized with 5% trichloroacetic acid (TCA). The supernatants were neutralized with 2.5 M potassium hydroxide/1.5 M K_2HPO_4 and stored at -20°C

until further use. UDP-GlcNAc was determined by HPLC using a CarboPac PA1 column (250x4mm, Dionex) and a guard column (4x50mm) of the same material. Analytes were eluted using an ammonium acetate gradient (Zhang, Zhou, Bao, & Liu, 2006) with detection at 262 nm. Under these conditions UDP-GlcNAc elutes with a retention time of 15.3 min (Namboori & Graham, 2008). The UDP-GlcNAc concentrations in cell extracts were calculated from the integrated peak areas using appropriate standards and the data was normalized based on total cell dry weight measured according to Namboori *et al*. (Namboori & Graham, 2008). Experiments were carried out in triplicates with independently prepared cell extracts.

Results

IDENTIFICATION OF THE P_{RRAB} PROMOTER

Analysis of the DNA sequence upstream of the *rraB* gene using the GENETYX-MAC (11.2.5) software suggested the existence of two putative promoters that match the δ^{70} consensus -35 and -10 sequences. The proximal promoter has -35 and -10 sequences centered at 128 and 104 nucleotides, respectively, upstream of the rraB translation start site (Figure 2.1A). The upstream region containing this putative promoter sequence is well conserved ($\geq$80% sequence identity) among γ-proteobacteria including *Escherichia coli, Shigella flexneri* and *Salmonella enterica*. (Figure 2.1B).

Northern blot analysis with *rraB*-specific probes revealed that the *rraB* mRNA is transcribed throughout the exponential and stationary phase (Figure 2.2). A single band

corresponding to a transcript of approximately 500 bases was detected suggesting that transcription of *rraB* occurs from the putative proximal promoter and gives rise to a monocistronic mRNA. Primer extension of RNA isolated from E. coli JCB570 revealed a single *rraB* transcript that is initiated at a T residue 88 bp upstream from the ATG codon (Figure 2.1C). This promoter was designated P_{rraB}.

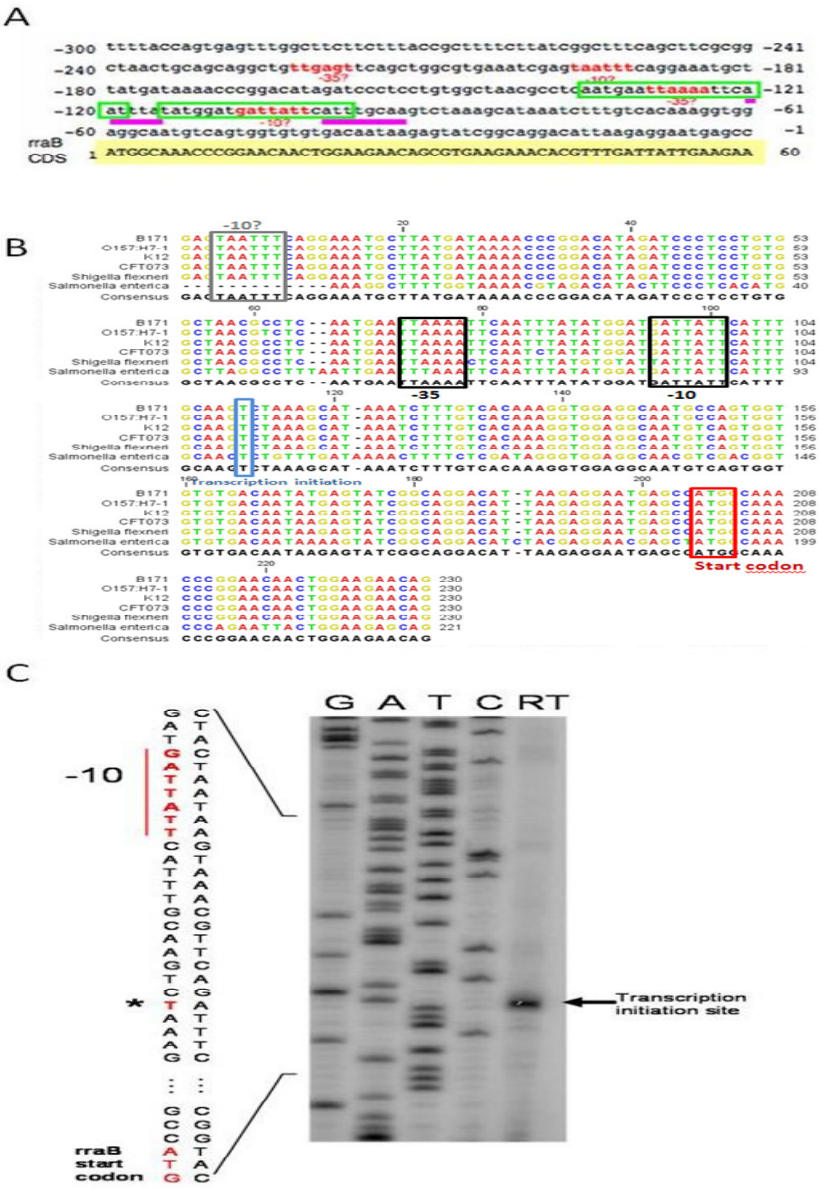

Figure 2.1: Identification of PrraB (A) Two pairs of putative promoters that match the δ^{70} consensus -35 and -10 sequences were identified using GENETYX-MAC 11.2.5. The arginine repressor binding sites (ARG boxes) are shown boxed, the *argI* promoter sequence is underlined and the *rraB* coding sequence is highlighted. (B) Multiple sequence alignment of the argI-rraB intergenic sequence: Abbreviations: B171, *Escherichia coli* B171, O157:H7-1, *Escherichia coli* O-157, K12, *Escherichia coli* K-12, CFT073, *Escherichia coli* CFT073. The transcription start codon, upstream putative -10 site, proximal -35, and -10 sites are shown in boxes. (C) Primer extension

analysis. Asterisk and arrow showed transcription initiation site and the reverse transcription product respectively.

The promoter activity of P_{rraB} was further analyzed using *lacZ* transcriptional fusions. The different regions upstream of rraB extending up to the putative distal promoter as shown in Figure 2.3A, were amplified by PCR and cloned upstream of the *lacZ* gene in the low copy transcriptional fusion vector, pSP417 resulting in plasmids pMZB002 {Φ (-239 to -1) *rraB-lacZ*}, pMZB003{Φ(-152 to -1) *rraB-lacZ*}, and pMZB004 {Φ (-239 to -153) *rraB-lacZ* }. To rule out the possibility that differences in the β-galactosidase activity expressed from the above transcriptional fusions might be partially due to plasmid copy number effects, the *lacZ* fusions were inserted into the chromosome. (Simons, Houman, & Kleckner, 1987) First, the *lacZ* fusions were transferred into either λRS74 or λRS45 via a double recombination event and then E. coli EC-O was lysogenized with the recombinant lambda phages to generate strains carrying a single copy of the respective promoter-*lacZ* fusion. As shown in Figure 2.3B, strain MZB003 {EC-O, λΦ(-152 to -1) *rraB-lacZ* }, encoding the *rraB* upstream region that includes the proximal promoter fused to *lacZ*, showed similar levels of β-galactosidase activity to those observed in MZB002 {EC-O, λΦ (-239 to -1) *rraB-lacZ*}, which contains a fusion to the rraB upstream region including both the proximal and the distal putative promoter sequences. In contrast, MZB004 {EC-O, λΦ (-239 to -153) *rraB-lacZ*} containing a fusion to the *rraB* upstream region that lacks the proximal promoter gave background activity. These results further support the notion that *rraB* is transcribed from the

proximal promoter, P_{rraB}. In the studies described below, the transcriptional fusion, λΦ (-152 to -1) *rraB-lacZ* is now designated as Φ (P*rraB-lacZ*).

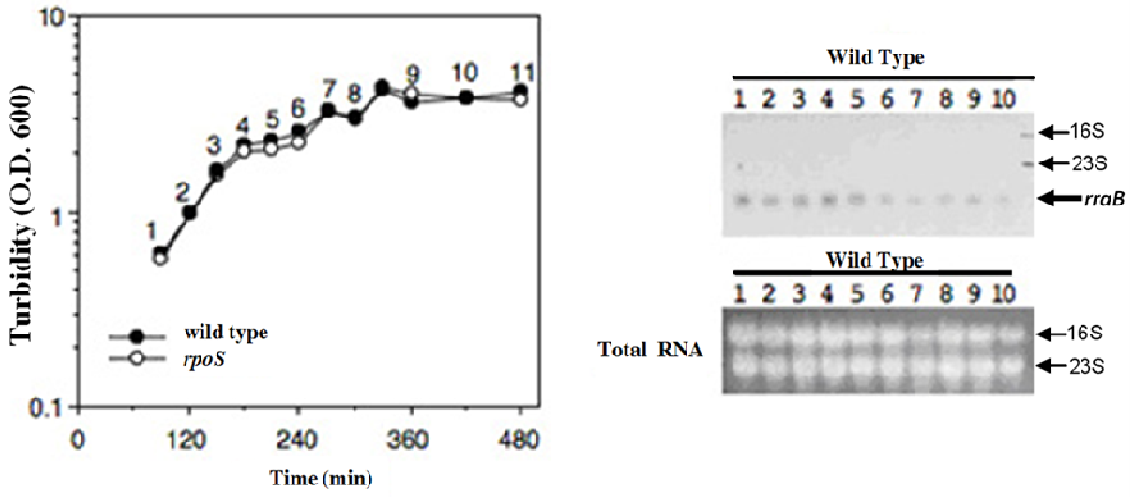

Figure **2.2**: Northern Blotting of rraB gene in strain JCB570 (upper right panel), total RNA (lower right panel) and growth curve with sampling times for RNA isolation (left panel). The *rraB* transcript is about 500 bases in length.

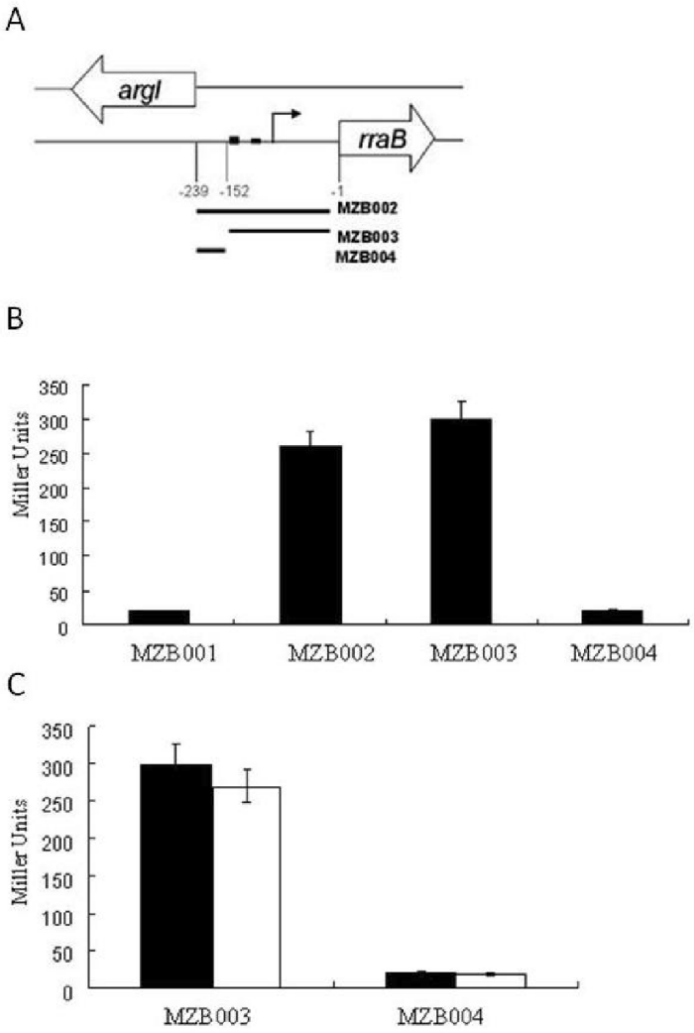

Figure 2.3: Transcriptional LacZ fusions (A) Schematic of the transcriptional *rraB –lacZ* fusions used in this study. (B) and (C): β-galactosidase activities in MZB001, MZB002, MZB003 and MZB004 cells. Cells were grown in LB under aeration at 37°C, and harvested in either log phase (A_{600} = 0.5, shown in black) or stationary phase (A_{600} = 1.6, shown in white). Samples were normalized by A_{600} and enzymatic activities were measured in Miller units. The data presented are the average of at least three independent determinations and the error bars correspond to the standard deviation.

The expression of the *rraA* gene was previously shown to be induced in stationary phase.(Zhao, Zhou, Kawarasaki, & Georgiou, 2006) Northern blot analysis (Figure 2.2) and measurements of the β-galactosidase activity expressed from the Φ(P*rraB-lacZ*) fusion in exponential and stationary phase cells revealed that the transcription level of *rraB* is not affected by the growth phase (Figure 2.3C). The E. coli *rraB* gene is adjacent to *argI* which is transcribed from the opposite strand and encodes ornithine carbamoyltransferase I, a key enzyme in arginine biosynthesis. Earlier microarray analyses had indicated that the expression of *rraB* is correlated with that of *argI* and it is increased upon arginine deprivation (Khodursky et al., 2000, Ramelot et al., 2003). Interestingly, the genomic organization of *rraB* and *argI* is conserved in other γ-proteobacteria such as *S. enterica* and *Y. pestis.* In *V. cholerae*, the *rraB* homologue, VC0424 is located in a similar head-to-head orientation with VC0423 (Figure 2.4), which codes for arginine deiminase that is involved in arginine catabolism. Inspection of the nucleotide sequence in the *argI-rraB* intergenic region revealed the presence of a putative arginine repressor (ArgR) binding site (ARG box), which consists of two neighboring 18-bp palindromic sequences separated by three nucleotides (Figure 2.1A). The influence of arginine availability on *rraB* transcription was examined as follows: First, excess arginine (20 mM) was added to cultures growing in minimal medium. Second, cells grown in LB were transferred into medium without arginine for two hours to achieve transient arginine starvation. Neither excess nor depletion of arginine exerted any significant effect on the β-

galactosidase activity of MZB003 cells carrying the Φ(P_{rraB}-*lacZ*) fusion (data not shown).

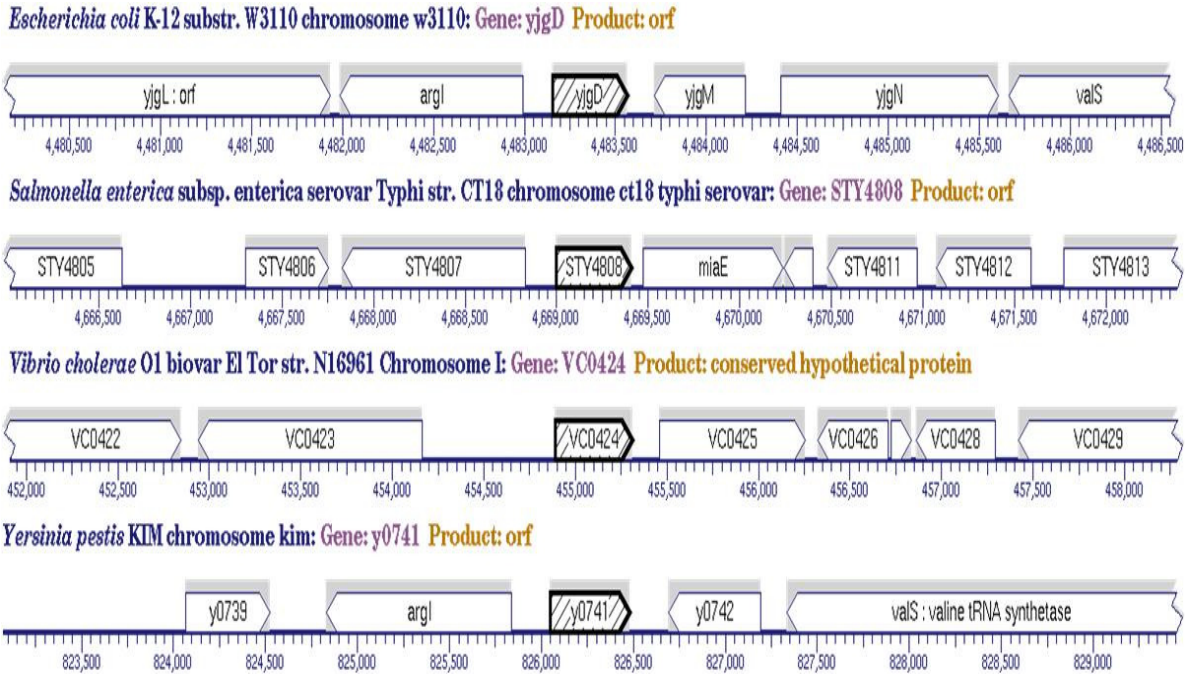

Figure 2.4 Multi-Genomes ortholog analysis (http://www.biocyc.org) showing the head-to-head alignment of *rraB* (*yjgD*) and *argI* conserved in *E. coli* and related bacteria. STY4807 in *S. Typhi* coding for ornithine carbamoyltransferase subunit I and VC0423 in *V. cholera* coding for arginine deiminase, are both involved in L-arginine metabolism pathways.

Khodursky *et al.* reported that the expression of the *rraB* gene is repressed in response to tryptophan starvation (Khodursky et al., 2000). To evaluate the effect of tryptophan on the transcriptional activity from P_{rraB}, we determined the β-galactosidase activity in MZB003 grown either in minimal media with excess tryptophan or under conditions of tryptophan starvation (data not shown). None of these conditions affected the level of

β-galactosidase activity expressed from the Φ(P_{rraB}-*lacZ*) fusion, indicating that P_{rraB} promoter does not respond to tryptophan availability.

TRANSPOSON MUTAGENESIS

Transposon mutagenesis and screening for colonies displaying a higher level of β-galactosidase activity from the Φ(P_{rraB}-*lacZ*) fusion were employed to isolate chromosomal lesions that might result in increased transcription from the P_{rraB}. First, the Φ(P_{rraB}-*lacZ*) fusion was transferred into the Δ*lac* strain P90C resulting in strain LZ001, which gave pale blue colonies on LB agar plates containing 25 μg/ml X-gal. Following transposon mutagenesis using the EZ-Tn5^{TM} transposome, six dark blue colonies were isolated from approximately 32, 000 colonies tested. One of these colonies, designated LZ002, reproducibly produced the dark blue phenotype on X-Gal plates and also resulted in higher β-galactosidase activity in lysates from cells grown in liquid cultures. Genomic DNA from LZ002 was purified, digested with EcoRI, self-ligated and transformed into the *E. coli pir+* strain BW21116 (Haldimann, Daniels, & Wanner, 1998). The colonies formed on kanamycin plates carry plasmids made of circular genomic DNA fragments containing the Tn*5* insertion. Plasmid DNA was isolated and the site of the transposon insertion was determined by DNA sequencing using transposon-specific primers. This analysis revealed that the transposon insertion occurred at 391, 0475 bp of the E. coli chromosome, which corresponds to the nucleotide 852 in *glmS* (Figure 3A). *glmS* encodes the enzyme L-glutamine: D-fructose-6-phosphate

amidotransferase (EC 2.6.1.16), also known as GlcN-6-P synthase. GlcN-6-P synthase is a critical metabolic control point in the biosynthesis of amino sugar-containing macromolecules. It catalyzes the first committed step in the pathway leading to the formation of UDP-GlcNAc, a universal GlcNAc donor for the biosysthesis of cell walls, extracellular matrix, glycolipids and the protein posttranslational modifications (Milewski, 2002; Namboori & Graham, 2008).

The *glmS852::*Tn*5* strain LZ002 grew slower than the parental wild-type strain in both rich (data not shown) and minimal media (Figure 2.5B). LZ002 displayed four-fold higher β-galactosidase activity than its isogenic control LZ001 in exponential phase (Figure 2.5C). Consistent with this result, the steady-state level of *rraB* mRNA as determined by real time RT-PCR was five-fold greater in *glmS852::*Tn*5* cells compared to the parental strain LZ001(Table 2.2). To rule out the possibility that the increase in transcription from the P_{rraB} promoter in cells containing the *glmS852::*Tn*5* allele was related to their lower growth rate, I also compared the steady state *rraB* transcript level in strain Mjf256.10 (Faulkner, Veeravalli, Gon, Georgiou, & Beckwith, 2008) which grows at a comparable rate to LZ002 as a result of mutations that affect the cytoplasmic reduction pathways and are unrelated with UDP-GlcNAc metabolism. In contrast to the 5-fold increase observed in the *rraB* mRNA levels of LZ002 relative to its parental strain, the *rraB* transcription in strain Mjf256.10 was slightly lower (67%) than that of its parental strain DHB4 as determined by real time RT PCR.

To test whether specific complementation of glmS can reverse the effect of *glmS852::*Tn*5* mutation, glmS was cloned into a low-copy plasmid, pBAD30, and expressed from an arabinose-inducible promoter. When grown in M9 minimal medium supplemented with 0.2% glucose but without arabinose, LZ002 cells transformed with pBAD30-*glmS* exhibited similar β-galactosidase activity as LZ002 cells without plasmid (data not shown). However, when the strain LZ002 containing pBAD30-*glmS* were grown in the presence of 0.2% of arabinose, the β-galactosidase activity was reduced to the level observed in the parental strain LZ001. Under these conditions cells containing pBAD-*glmS* accumulate GlmS at the level comparable to that obtained from the chromosomal copy of glmS in the parental Stain LZ001, as monitored by Western blotting using anti-GlmS antibodies (data not shown). As a control, transferring the empty pBAD30 plasmid did not reverse the effect of *glmS852::*Tn*5* mutation under both growth conditions (Figure 2.5D). Moreover, consistent with the physiological role of GlcN-6-P synthase, addition of its enzymatic reaction end product (GlcN-6-P) to LZ002 cells resulted in normal growth rate (Figure2.6) and basal β-galactosidase activity (Figure 2.5C). Finally, the *glmS852::*Tn*5* allele did not affect the LacZ activity from a chromosomal (P_{rraA}-*lacZ*) fusion (Zhao, Zhou, Kawarasaki, & Georgiou, 2006) indicating that the impairment of glmS specifically enhances the transcription of *rraB* but not of the other RNase E inhibitor, *rraA* (data not shown).

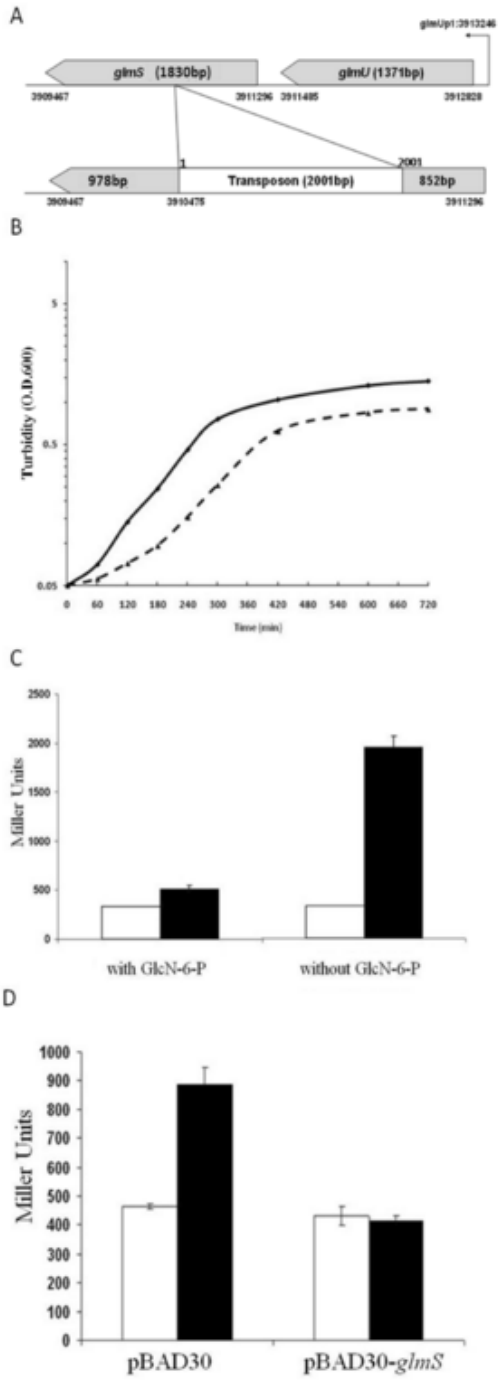
A
glmU/p1:3913246
glmS (1830bp)
glmU (1371bp)
3909467
3911296
3911485
3912828
1
2001
978bp
Transposon (2001bp)
852bp
3909467
3910478
3911296
B
Turbidity (O.D.600)
5
0.5
0.05
0
60
120
180
240
300
360
420
480
540
600
660
720
Time (min)
C
Miller Units
2500
2000
1500
1000
500
0
with GlcN-6-P
without GlcN-6-P
D
Miller Units
1000
900
800
700
600
500
400
300
200
100
0
pBAD30
pBAD30-glmS

Figure 2.5: A transposon insertion in *glmS* upregulates *rraB* (A) Location of the transposon insertion in the *glmS* gene. *glmS* is cotranscribed with upstream *glmU* from promoter *glmU*p1. (B) Growth curve of strains LZ001 (in solid line) and LZ002 (*glmS852::*Tn*5*, in dashed line) cultured in M9 media with 0.2% glucose. (C) -galactosidase activities in strains LZ001(white) and LZ002 (black) in the presence or absence of 20 μg/ml GlcN-6-P were measured in cells grown in M9 media and harvested at A_{600} = 0.2-0.3. (D). Complementation of the *glmS852::*Tn*5* mutation with plasmid pBAD-*glmS*. *E.coli* strains LZ001 (white) and LZ002 (black) transformed with plasmid pBAD30 or pBAD30-*glmS* as indicated were grown overnight in M9 with 0.2% glucose and subcultured into fresh M9 media with 0.2% glycerol. At A_{600} = 0.4-0.5, 0.2% arabinose was added. Cells were harvested 2 hours after induction and the -galactosidase activity was determined.

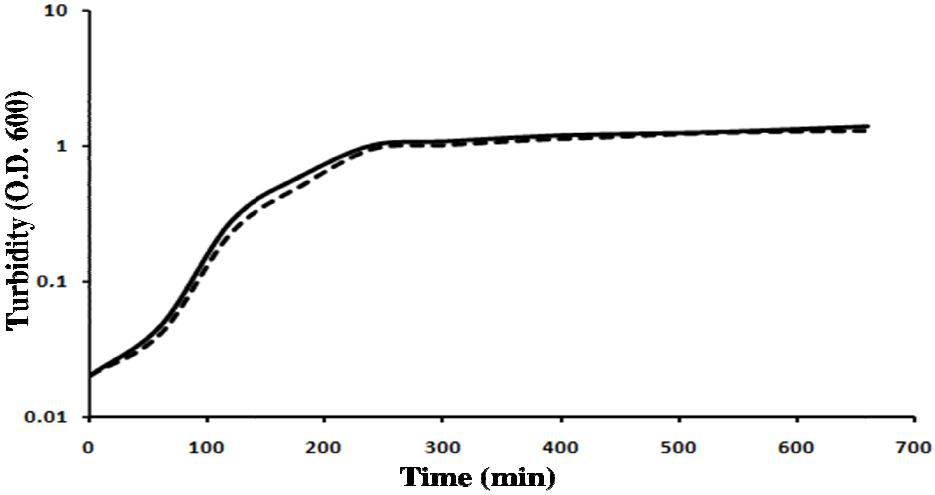

Figure 2.6 Growth curve of *E. coli* strain LZ001 (solid line) and LZ002 (dashed line) in M9 medium supplied with 20μg/ml GlcN-6-P.

Because of the importance of *glmS* in cell wall synthesis and its related pathways, we speculated that *rraB* is involved in cell envelope stress response. I tested the effect of deletions in *dsbA*, *degP* and *rseB/degS* which are known to cause cell envelope stress (Bessette, Qiu, Bardwell, Swartz, & Georgiou, 2001, Strauch, 1988, (Grigorova et al., 2004) on P*rraB* transcription by introducing these mutations to strain LZ001 using P1

transduction. None of them shows significant effect the P*rraB* activity based on β-galactosidase activity (Figure 2.7).

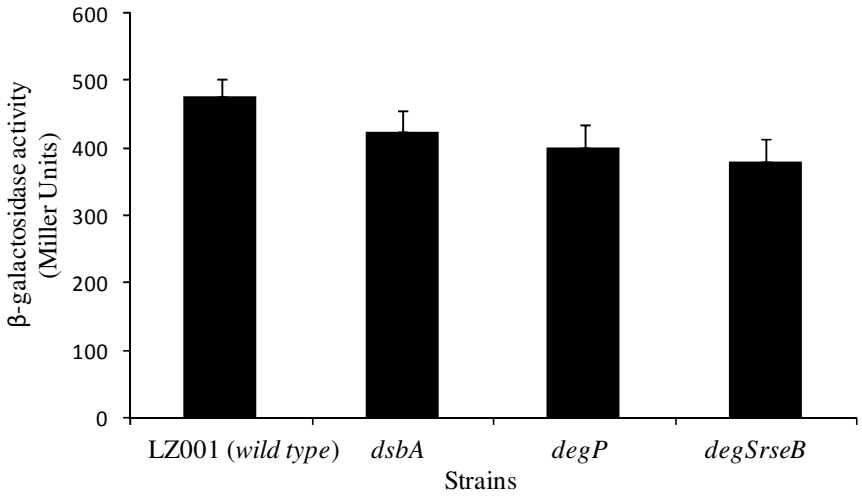

Figure 2.7 β-galactosidase activities from strain LZ001 and its mutant strains carrying deletions in genes that induce envelope stress. Mutations in dsbA, degP or in degS and rseB were transferred into LZ001 by P1 transduction from different strains (Table 1). β-galactosidase activities were measured in cells grown in M9 media with 0.2% glucose and harvested at A_{600} = 0.2-0.3.

EFFECT OF *GLMS852::*TN*5* MUTATION ON *RNE-LACZ* ACTIVITY

RNase E autoregulates its expression in *cis* by cleaving its own mRNA near the 5′ UTR region. Consequently, the production of RNase E is inversely affected by changes in the catalytic activity of the enzyme. Strain CJ1825 (MC1060, *λez1*) contains a chromosomal fusion of truncated *rne* gene (the 5′ UTR of rne gene, and N-terminal 181 codons) linked to the *lacZ* reporter. Due to the self-cleavage of the rne-lacZ transcript, a higher β-galactosidase activity in strain CJ1825 indicates a decrease in RNase E activity and *vice*

versa (Jain & Belasco, 1995). We previously showed that over expression of RraB conferred increased β-galactosidase activity from the *rne-lacZ* of this strain (Gao et al., 2006). We examined whether the *glmS852::*Tn*5* allele and the resulting upregulation of *rraB* also inhibit RNase E, in turn give rise to a higher β-galactosidase activity. The *glmS852::*Tn*5* mutation was introduced into strain CJ1825 via P1 transduction to give rise to *E.coli* LZ003. The *glmS852::*Tn*5* allele in *E.coli* LZ003 also caused a growth defect in both rich and minimal media (data not shown). -galactosidase activity was increased by more than 2-fold in LZ003 compared to wild type (Figure2.8). Notably the observed increase in β-galactosidase activity from the *rne-lacZ* fusion in strain LZ003 is comparable to that obtained through over expression of *rraB* transcribed from a trc promoter in plasmid pTrc99a (Gao et al., 2006).

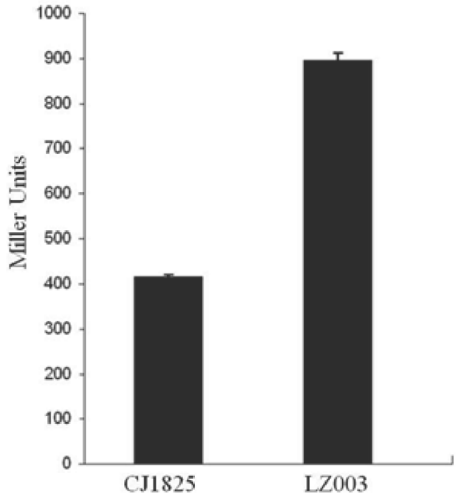

Figure 2.8 The *glmS852::*Tn*5* allele reduces β-galactosidase activity from the *rne-lacZ* fusion. *E. coli* strains CJ1825 and LZ003 were cultured in LB media. At log phase, cells were harvested and the β-galactosidase activities were determined.

Discussion

In earlier studies we showed that RraB is a protein inhibitor that interacts with RNase E, modulates the composition of the degradosome and affects the ability of the RNA degrading machinery to recognize and cleave numerous RNAs. Studying the regulation of *rraB* gene expression is important for understanding its physiological significance. Primer extension and *lacZ* transcriptional fusion experiments demonstrated that *rraB* is transcribed from its own promoter (P_{rraB}) located 88 bp upstream from the translation start codon. Northern blot analysis and *lacZ* transcriptional fusion experiments demonstrated that, unlike *rraA*, the transcription of *rraB* is not growth phase-dependent. The *E. coli rraB* and its homologues in other bacteria, such as *S. typhimurium, Y. pestis* and *V. cholerae*, are arranged in a head-to-head alignment with the adjacent gene, *argI*. Simultaneous regulation of two divergent promoters by ArgR has been described for a number of adjacent gene pairs such as *argE* and *argC* or *argG* and *metY*. (Krin, Laurent-Winter, Bertin, Danchin, & Kolb, 2003) While the existence of a putative ArgR binding site suggests that transcription from P_{rraB} might be regulated by the availability of L-arginine, we observed that the transcriptional activity as determined from the level of β-galactosidase, was unaffected by the presence or absence of L-arginine. Similarly we found that transcription of P_{rraB} is not affected by tryptophan starvation, inconsistent with earlier microarray analysis (Khodursky et al., 2000, Ramelot et al., 2003). Because in microarray studies the steady state mRNA level is the outcome of both transcriptional regulation and post-transcriptional effects, the observed correlation between the mRNA

levels of tryptophan/arginine metabolic genes and *rraB* in those studies could be related to *rraB* mRNA itself or other post transcriptional regulations, rather than its promoter.

Transposon mutagenesis was employed to identify transcriptional regulators of *rraB* promoter by screening for enhanced β-galactosidase activity from the Φ(P_{rraB}-*lacZ*) transcriptional fusion. Screening of over 30,000 colonies led to the isolation of one clone (LZ002) which displayed 4 fold higher β-galactosidase activity, and moreover, a 5-fold greater steady state accumulation of the *rraB* transcript. Surprisingly, the transposon insertion was located in the *glmS* gene encoding the essential enzyme GlcN-6-P synthase, a ubiquitous protein, present in all known organisms. Both prokaryotic and eukaryotic enzymes contain an N-terminal glutamine-binding domain and a C-terminal D-fructose-6-phosphate-binding domain, with the eukaryotic enzymes having additional 40–90 amino acid residues linking the two. Except for the eukaryotic linker region, the N-terminal and C-terminal domains are highly conserved, including all the residues involved in substrate binding and catalysis (Milewski, 2002). We found that in strain LZ002, the Tn5 transposon was inserted in the C-terminus after the conserved N-terminal domain. Upon further inspection, we noticed the existence of a putative start codon at the 3 of Tn5, which is preceded by an AU rich sequence 15 nt upstream that might serve as a ribosomal binding site for the translation of a chimera comprising the C-terminal part of GlmS. According to this hypothesis, the transposon insertion might result in the synthesis of two GlmS polypeptides, one comprising the N-terminal 284 amino acids and the second comprising amino acids 285-620. Early studies of GlmS showed that

chymotrypsin cleaves this protein at Tyr240 within a flexible loop to produce an N-terminal glutamine hydrolase domain and a C-terminal fructose-6-phosphate isomerase domain; however the reconstituted protein fragments do not catalyze the full GlcN-6-P synthase reaction (Denisot, Le Goffic, & Badet, 1991). The additional amino acids 241-284 in the present construct form α-helices 7 and 8, which could interact with helices of the isomerase fragment to form a stable SIS domain (Teplyakov, Obmolova, Badet, & Badet-Denisot, 2001). Interaction between the two subunits would form an ammonia channel, conferring weak glucosamine-6-phosphate synthase activity, in turn enabling the synthesis of essential UDP-GlcNAc. Because the cellular level of GlcN-6-P is beyond detection limit, to evaluate this hypothesis we determined the cellular concentration of UDP-GlcNAc in the *glmS852*::Tn*5* strain LZ002 and its isogenic control LZ001 using HPLC (Namboori & Graham, 2008). As expected, LZ002 was found to synthesize UDP-GlcNAc, but at a reduced level. The concentration of UDP-GlcNAc in mutant strain was 53% lower than that in the parent strain (LZ002 versus LZ001, respectively) with a statistically significant difference of $p<0.01$ (2 tailed t-test).

These results indicate that these cells have a functional GlcN-6-P synthase, possibly resulting from the translation of the C-terminal fragment, which in combination with the N-terminal polypeptide can reconstitute the active enzyme. Regardless of the mechanism that mediates the synthesis of GlcN-6-P, our results indicate that the transcription of rraB is modulated either by GlcN-6-P or by other metabolites derived from GlcN-6-P. This

effect is not the result of the reduced growth rate conferred by the *glms852::*Tn*5* allele, nor does it affect the other RNase E inhibitor *rraA*, indicating that it is specific to *rraB*.

As the enzyme catalyzing the first committed step of the UDP-GlcNAc pathway that provides the building blocks for the formation of cell wall macromolecules, GlcN-6-P synthase is an obvious point of metabolic control. According to Collins et al. (Collins, Irnov, Baker, & Winkler, 2007), in *B. subtilis*, the 5′ UTR of the *glmS* messenger RNA contains a metabolite-sensing ribozyme. Binding of GlcN-6-P to the ribozyme stimulates autocatalytic site-specific cleavage near the 5′ of the transcript, resulting in the degradation of the transcript by RNase J1. Interestingly, RNase J1 is the endoribonuclease in *B. subtilis* with functional homology to RNase E in *E. coli* except that RNase J1 specifically cleaves transcripts with 5′ hydroxyl groups (Collins, Irnov, Baker, & Winkler, 2007). Kalamorz and Reichenbach (2007) reported that the regulation of *glmS* by GlcN-6-P in *E. coli* differs substantially from *B. subtilis*: in *E. coli*, when the intracellular GlcN-6-P concentration decreases, the short form of small RNA GlmY (GlmY*) accumulates and acts to stabilize a second small RNA, GlmZ, which is a homolog of GlmY. GlmZ is derived from the processing of the *glmUS* primary transcripts by RNase E and can stabilize *glmS* trancripts in concert with protein YhbJ (Kalamorz, Reichenbach, März, Rak, & Görke, 2007; Reichenbach, Maes, Kalamorz, Hajnsdorf, & Görke, 2008). Moreover, the *glmS* mRNA generated by RNase E from *glmUS* transcript is highly susceptible to poly (A)-dependent degradation (Joanny et al., 2007). We found that the *glmS852::*Tn*5* allele increased *rraB* transcription, thereby lowering the RNase E

activity. These findings raise the possibility that upregulation of *rraB* in response to changes in metabolites of the GlcN-6-P pathway results in a reduction in RNase E activity, which in turn affects the processing of the *glmUS* primary transcripts. Thus, as with other post-transcriptional mechanisms of regulation, RraB may facilitate rapid alterations in RNA decay and/or processing in response to specific environmental stimuli such as reduced cellular levels of GlcN-6-P. The mechanism by which mutations that reduce GlcN-6-P synthase activity affect RraB expression and its detailed effect on the processing of the *glmUS* transcript are subjects of on-going studies.

Part of this chapter is adopted from a previous publication:

(Zhou, Zhao, Wolf, Graham, & Georgiou, 2009)

CHAPTER 3 RECONSTITUTION OF RNA DEGRADOSOME *IN VITRO*

Introduction

The RNA degradosome was discovered in 1994 by Carpousis *et al.* during the purification of RNase E. The major components of this complex were shown to be RNase E, RhlB, Pnpase and Enolase. Since then this complex has been the subject of

intensive study regarding its organization, structure and function. The mostly unstructured C terminal portion of RNase E serves as a platform where the degradosome is assembled. Using C terminal fragments of RNase E, the binding site of RhlB, Pnpase, and Enolase have been mapped. Ben F. Luisi *et al.* have solved the structures of each of these enzymes in the presence of their corresponding RNase E binding peptides. Structural information along with kinetic analysis revealed cooperativity effects between these components. This information was summarized in Chapter 1 of this dissertation.

The majority of earlier studies were performed using pulled down complexes or fragments of proteins. This is because the C terminal of RNase E is highly unstructured and susceptible to degradation during purification. To reconstitute the *E.coli* RNA degradosome, Worrall and Gorna *et al.* used modular coexpression vectors, with one plasmid containing RNase E and RhlB and, a second plasmid containing Enolase and Pnpase. Using this method, all four components of the degradosome could be expressed and purified, effectively protecting the C-terminal. This approach has several shortcomings: First of all it is not possible to rule out the presence of truncated RNase E in these preparations; second the purified complex contains contaminating OmpT; third the complex may also contain RNA impurities; finally the co-elution of all four components does not allow kinetic analyses with different ratios of individual enzymes (Worrall et al., 2008).

To this end, we have cloned expressed and purified the four major components of the RNA degradosome. Proteolysis was reduced by employing a denaturing purification

technique. Immunoprecipitation experiments showed that the refolded proteins were able to re-form a complex *in vitro*. All four components of the RNA degradosome were produced at biochemical relevant amounts and satisfying purity for future kinetic assays. Furthermore, the interaction between different components was determined. This chapter describes the biochemical evidence of an *in vitro* degradosome formation and the functional study of such complex with regard to RNase E inhibitors RraA and RraB is the subject of chapter 4.

Materials and Methods

BACTERIAL STRAINS, PLASMIDS AND GROWTH CONDITIONS

The plasmids used in this study are listed in Table 3.1. The C-terminal His-tagged truncated RNase E expression plasmids were constructed as follows: *rne* gene fragments were PCR amplified. PCR products were digested with BsaI/XhoI and cloned into pET28(a) as previous described (Gao et al., 2006). The C-terminal SPA tagged degradosome components: *rhlB, pnp* and *eno* were PCR amplified from an E. coli SPA-Tagged Strain (Open Biosystems, AL), restriction enzyme digested using NdeI and HindIII moved into the pET21(a) expression vector. The *rraA* and *rraB* genes were PCR amplified from genomic DNA of wild type *E.coli* strain JCB570 (Zhao, Zhou, Kawarasaki, & Georgiou, 2006), subjected to digestion with NdeI/BlpI and cloned into pTrc99A with N terminal 6xHistidine tags.

Table 3.1 Plasmids used in this study

plasmids	Description	Reference or Source
pET28(a)	fl ori, Kan r T7 expression vector, C-terminal 6x Histidine tag	Novagen
pET28(a)-Rne845	*rne845* under T7lac promoter in pET28(a)	This study
pET28(a)-Rne1045	*rne1045* under T7lac promoter in pET28(a)	This study
pET21(a)	fl ori, Amp r T7 expression vector	Novagen
pET21(a)-Eno-SPA	*eno*-SPA under T7lac promoter in pET21(a)	This study
pET21(a)-RhlB-SPA	*rhlB*-SPA under T7lac promoter in pET21(a)	This study
pET21(a)-Pnp-SPA	*pnp*-SPA under T7lac promoter in pET21(a)	This study
pTrc99A	Expression vector; Ampr Ptrc rrnB TtT2 ori (pBR322) lacIq	Amersham Pharmacia Biotech
pTrc99A-H-RraA	*rraA* under trc promoter with N terminal 6x Histidine tag in pTrc99A	This study
pTrc99A-H-RraB	*rraB* under trc promoter with N terminal 6x Histidine tag in pTrc99A	This study
pIDTSMART-T7RNA1	T7 promoter sequence followed by RNA1 cDNA template cloned with flanking EcoRI sitesin pUC ori plasmid, KanR	This study

PROTEIN EXPRESSION AND PURIFICATION

For purification of truncated RNase E proteins, pET28(a) plasmids harboring appropriate gene fragments were transformed into the E. coli strain BL21(DE3). Bacteria cultures were grown in TB (Terrific broth) media at 37 °C to optical density (measured at A_{600}) of approximately 0.5. Protein expression was induced with 1mM isopropyl--D-thiogalactopyranoside (IPTG), and then cells were incubated for an additional 4-6 hours at 37 °C. The RNase E (residues 1-1045) protein with a C-terminal Histidine tag was

purified under denaturing conditions using the Ni2+-nitrilotriacetic acid-agarose (Qiagen, CA) affinity column as follows: Cell pellets were suspended in denaturing lysis buffer (100 mM NaH_2PO_4, 8M Urea, and 10 mM Tris-HCl, pH 8.0) with 0.5% TritonX-100. Complete protease inhibitor cocktail tablets (Roche, IN) were added to all purification buffers according to the manufacturer′s instructions. The 10x cell resuspensions were passed through a French press (Thermo electron, MA) twice at 20,000 psi to promote cell lysis. The cell lysates were clarified by centrifugation and filtration. Filtered supernatants were mixed with Ni^{2+}-nitrilotriacetic acid-agarose previously charged and equilibrated with lysis buffer with 10mM imidazole. Following binding for 3 hours at room temperature, the slurry was packed into a column and washed with 10 column volumes of lysis buffer with 10 mM imidazole. An imidazole concentration gradient (in lysis buffer) ranging from 25mM to 250mM was applied for protein elution. The majority of the RNase E protein eluted at concentrations between 100 and 250mM imidazole. The eluant was then dialyzed into RNase E storage buffer (50mM Tris-HCl, 1mM EDTA, 500mM NaCl, 20% (v/v) glycerol, 0.5% Triton X -100, and 1mM DTT) at 4 ºC overnight. The refolded protein was concentrated by Amicon Ultra Ultracel-100K centrifugal filter. (Millipore, MA).

The C-terminal SPA tagged Pnpase was purified from BL21(DE3) strains carrying pET21a-Pnp-SPA construct using anti-FLAG M2 beads (Sigma, MO) according to manufacturer′s instructions. The eluted protein (in Glycine Tris-HCl buffer with protease inhibitor) was dialyzed into RNase E storage buffer at 4 ºC overnight and concentrated

using Amicon Ultra Ultracel-30K centrifugal filter devices. RhlB and enolase proteins were purified following the same procedure as Pnpase. All proteins used in this study were more than 95% pure as determined by Gelcode bluestained (Thermo, MA) SDS PAGE. The final protein concentrations were determined by Nanodrop® ND-1000A (Thermo Scientific, DE) at their corresponding molecular weights and extinction coefficients (protein calculator v3.3)

The RraA and RraB proteins were purified using similar approaches except that the host strain carrying the pTrc99A-RraA/RraB constructs was AC27 (MC1061, *rne(ams)*, *rne131 i.e.* the C-terminal *rne* (585-1061) truncation) instead of BL21(DE3). After elution, RraA and RraB proteins were concentrated and buffer exchanged into low salt buffer (20mM Tris-HCl, pH7.5) using Amicon Ultra Ultracel-10K centrifugal filter devices. (Millipore, MA). The concentrated protein solutions were then applied to a MonoQ HR5/5 anion exchange column (GE healthcare, UK). Proteins were eluted as 1 ml fractions using 35ml of 20mM Tris-HCl (pH7.5) and a salt gradient ranging from 0 to 1 M NaCl. The eluant was then dialyzed into RNase E storage buffer at 4 ºC overnight and concentrated again. The use of AC27 RNase E truncated strain coupled with the purification steps lowered nucleic acid and RNase contamination significantly to levels that did not influence subsequent kinetic analyses.

IMMUNOPRECIPITATION AND WESTERN BLOTTING

2 μM of C-terminal truncated RNase E (1-845 residues) with a Histidine tag, and different amounts of enolase or RhlB were incubated with 10ul of Ni-NTA agarose

beads (Qiagen, CA) in binding buffer (150 mM NaCl, 10 mM imidazole, 10% glycerol, 50 mM Tris-HCl, pH 8.0) at 4 ºC for 1.5 hour with shaking (200 rpm). For co-precipitation of Pnpase in the presence of RhlB, 18μM of RNase E, 0-3 μM of RhlB and 1-4.5 μM of Pnpase were used in the binding step. The protein-bead mixture was centrifuged at 1500 rpm for 2 mins and washed thrice with 300 μl of washing buffer (150mM NaCl, 10mM imidazole, 10% glycerol, 1% NP-40, 50mM Tris-HCl, pH 8.0). After the final wash, Ni-NTA beads were collected and re suspended in 2x SDS PAGE loading buffer, proteins were resolved on an 8% SDS-PAGE. RNase E bands were detected by Western blotting with anti-Histidine-HRP conjugated antibody (Sigma, MO) diluted to a ratio of 1:2000. RhlB, Enolase and Pnpase were detected by Western blotting with anti-FLAG antibody (ECS HRP conjugated antibody, BETHYL, TX) diluted to a ratio of 1:10,000.

Results

PURIFICATION OF DEGRADOSOME COMPONENTS UNDER DENATURING CONDITION

The catalytic core (N-terminal 498 aa) of RNase E shares sequence homology to RNase G. This truncated RNase E has been the subject of numerous biochemical analyses using different RNA substrates. However, the lack of the C-terminus in this protein fragment makes it impossible to study the effect of other degradosome components on the processing of substrate RNAs by RNase E.

To date, almost all biochemical studies of RNase E function have been done with C-terminal truncated versions owing to the technical difficulties involved in the production and purification of full length RNase E. There are three major causes for these difficulties: First, as mentioned above, RNase E activity is tightly controlled *in vivo*. Over expression of RNase E and the subsequent increase in its activity is very detrimental to cell growth. Second, full length RNase E is very unstable and susceptible to proteolytic degradation during the purification process. Finally, RNase E is a membrane associated protein attached to the inner membrane and this complicates purification. To overcome these problems, our lab constructed vectors for the expression of various truncated versions of RNase E protein containing the first 499aa, 752aa, or 845aa as well as the 1045aa near full length enzyme (lacking the 16 C-terminal aa). We found that the 499aa and 752aa truncated versions were very easy to purify under native conditions. Longer proteins expressed from a T7 promoter however formed insoluble inclusion bodies. Therefore we sought to purify these proteins by refolding from denaturing conditions. Briefly inclusion bodies were dissolved in 7M urea, the detergent triton X-100 was added (0.1%) to increase solubility and the denatured protein was purified by Ni chromatography. The protein was then refolded by gradually dialyzed against the RNase E storage buffer as described in Methods. Using this procedure we obtained a of the RNase E 845aa fragment and of the full length RNase E of about 15 mg/liter culture and 5 mg/liter culture, respectively with a purity >90% as determined by SDS-PAGE (from an A_{600} of 2.0 culture) (Figure 3.1). It should be noted that the full length RNase E

protein migrates at about 200 kDa on a SDS PAGE despite possessing a molecular weight is about 120kD. This abnormal migration property is due to the Proline rich tails at the C-terminals of RNase E. (Cormack, Genereaux, & Mackie, 1993). In contrast to the full length protein the 845 aa truncated version of RNase E protein we generated does not show abnormal migration on SDS-PAGE.

For the other three major components of the RNA degradosome, we took advantage of previously constructed strain collection of *E.coli* strains encoding proteins tagged with a C-terminal SPA (sequential peptide affinity) tag, which contains three modified FLAG sequences and a calmodulin binding peptide (CBP) separated by a TEV protease cleavage site. Affinity chromatography using immobilized anti-FLAG antibodies was used to purify RhlB, Enolase, and Pnpase (Butland et al., 2005). The SPA tag enables us to detect these proteins using anti-flag antibody and to monitor complex formation *in vitro* as discussed below. Because of the high specificity and affinity of antigen binding, we were able to get very pure protein after one step affinity purification. The yield of RhlB and enolase using this purification system was about 15 mg/liter. The yield of Pnpase using this purification was about 20mg/ liter.

PROTEIN INTERACTION DETECTED BY *IN VITRO* IMMUNOPRECIPITATION

It is well established that those four proteins: RNase E, RhlB, Pnpase and Enolase form the degradosome complex *in vivo.* Pull-down assays using truncated RNase E mutants have mapped the different binding sites on the C-terminal of RNase E(Callaghan et al., 2004; Gao et al., 2006). We verified that purified proteins can interact *in vitro* and form

degradosome complexes by co-precipitation (pull down) experiments using Ni-NTA beads. Purified-N terminal 6xHistidine tagged RNase E 1-845aa protein were absorbed to Ni-NTA beads and incubated with RhlB or, enolase respectively. Following stringent washes to remove non-specifically bound protein to the beads, the resin was collected by centrifugation, resuspended in SDS-loading buffer and heat denatured. Samples were subjected to gel electrophoresis and immune blotting with anti-FLAG antibodies. An un-related 6xHistindine tagged IgG protein of the similar molecular weight as RNase E 1-845aa was used as a negative control (Data not shown).

The RNase E 1-845aa fragment which contains the RhlB and enolase binding sites were able to pull down C-terminal tagged RhlB and enolase respectively as expected, (Figure 3.1B top two panels). In the enolase experiment, we demonstrated saturation of Enolase binding: using 2 μM RNase E as bait, the amount of pulled down enolase is similar in reactions where the concentration of enolase was increased 2-fold from 7.5 to 15 μM. Previous *in vivo* pull-down assays demonstrated a binding ratio of enolase to RNase E between 1 and 2. Our data here is consistent with this estimate. It should be noted that the structure of enolase co-crystallized with RNase E binding peptide (Chandran & Luisi, 2006) C-terminal SPA tag should not interfere with the protein interaction between enolase and RNase E. It has been reported that the binding affinity between RNaseE and RhlB are within the 10 nM range. The *in vitro* pull down experiments using the 845 aa truncated RNase E and C-terminal SPA tagged RhlB in Figure 3.1B confirm this

interaction. Moreover, our data is consistent with a stoichiometric ratio between RhlB and RNase E binding which is 1:1 (monomer ratio).

RHLB ENHANCES PNPASE BINDING IN DEGRADOSOME

RhlB and Pnpase can form a strong complex *in vivo*. For several years, the β subunit of Pnpase was mistaken for enolase. It was not until 2005 that Lin Pei Hsun *et al.* rectified this assumption and proved that this degradosome subunit was actually RhlB (Lin & Lin-Chao, 2005) and that the two enzymes from a $\alpha_3\beta_2$ complex. We used size exclusion chromatography to confirm the formation of the complex of $\alpha_3\beta_2$ complex between RhlB and Pnpase. We also determined that Pnpase "piggy backs" onto RhlB to form a ternary Rnase E:RhlB:Pnpase complex with truncated RNase E lacking the Pnpase binding site. (1021-1061aa). As shown in Figure 3.1B lower panel, in the presence of RhlB, Pnpase can be pulled down by the 845 aa RNase E fragment. RhlB is required to promote the Pnpase pull down. In Fig 3.1 B RhlB and Pnpase can be differentiated based on their molecular weights difference. No such observe such "bridging" of "piggy back" effect was observed with Enolase. The amount of Pnpase that can be pulled down is dependent on RhlB consistent with the 2:3 stoichiometric ratio between Pnpase and RhlB reported earlier.

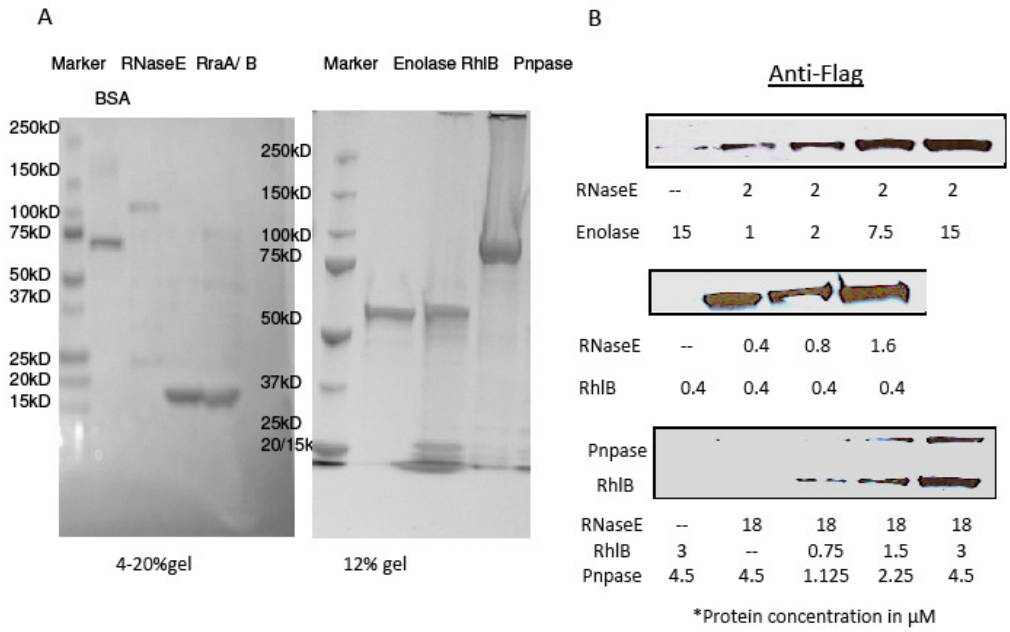

Figure 3.1 Purification results of recombinant degradosome proteins and *in vitro* immune precipitations of degradasome components by RNase E.
(A). N-terminal Histidine-tagged RNase E (1-1045aa.), RraA and RraB were purified as described in Methods and shown here on SDS-PAGE is an example of purified protein fractions after overnight dialysis (refolding) in RNase E storage buffer. C-terminal SPA tagged enolase, RhlB and Pnpase proteins were purified using anti-Flag agarose (Sigma, MI) affinity purification and dialyzed overnight in RNase E storage buffer. (B). Degradosome proteins co-precipitated using purified 845 aa RNase E fragment and Ni-NTA beads were analyzed by a western blot. Indicated amounts of protein were used in each co-precipitation reaction. The degradosome components proteins were C-terminal SPA tagged and detected by an anti-FLAG antibody as described previously. This *in vitro* experiment demonstrated the complex formation; moreover, it shows that the RNase E fragment exclude Pnpase binding site can pull down Pnpase via RhlB.

PURIFICATION OF RRAA AND RRAB TO REDUCE NUCLEASE CONTAMINATION

The isoelectric point (pI) of RraA and RraB proteins are 4.19 and 3.78 respectively, and therefore amenable to anion exchange chromatography purification. However, to investigate the effect of RraA and RraB on RNA degradation *in vitro*, it is critical to generate high quality protein devoid of any ribonuclease contamination. We found that prior to anion exchange chromatography nuclease treatment essentially eliminates contamination by negatively charged nucleic acids. Additionally we expressed these small proteins under a Trc promoter in pTrc99A vector in a strain lacking the C-terminal of RNase E to eliminate co-purification of RNase E. Finally the protein was purified by first denaturing with urea followed by IMAC chromatography under denaturing conditions and refolding prior to ion exchange chromatography. Incubation of the purified proteins with both short and long RNA substrates did not show any detectable RNase contamination under our experimental conditions.

Discussion

The major components of the *E. coli* degradosome are RNase E, RhlB, enolase and Pnpase. The structural and functional implications of the molecular interaction between these components have been the subjects of years of investigation. To date, the dissections of the C-terminal portion of RNase E that recruit the other degradosome components has been mapped (Callaghan et al., 2004; Gao et al., 2006). Likewise, the sites of interaction on RhlB, enolase and Pnpase have been illustrated along with the

crystal structures solved for these components bound to its corresponding RNase E peptides. ITC and SPR analysis has been applied to determine the dissociation constants for the protein interactions (Chandran et al., 2007; Chandran & Luisi, 2006; Nurmohamed, Vaidialingam, Callaghan, & Luisi, 2009). The RNase E peptide corresponding to RhlB binding site has been shown to activate RhlB by facilitating role RNA binding (Worrall, Howe, McKay, Robinson, & Luisi, 2008). The knowledge surrounding other functional interactions between degradosome is rudimentary at best. The overall significance of the 500-700 KDa degradosome complexes has been established three decades ago. However, little is known about the role of the individual components in RNA degradation, particularly with regards to the decay of different transcripts.

In order to biochemically analyze the complex by altering its composition, it is necessary to reconstitute the complex *in vitro* which requires the purification of individual degradosome components in substantial amounts (It is worth noting that this is also related to the sensitivity of the kinetic assay applied and its signal to noise ratio). However the full length RNase E protein which is the key component in organizing the RNA degradosome is a membrane-anchored protein that is prone to proteolytic degradation during purification. With the help of advanced protein purification techniques developed in our lab we have successfully purified milligram amounts of truncated versions of RNase E lacking only 16 aa from the C-terminal. The direct interaction between the truncated RNase E and purified RhlB or Enolase was illustrated

using *in vitro* immunoprecipitation. Intriguingly, the truncated RNase E lacking the Pnpase binding site (Segment D) pulls down Pnpase when RhlB is present. In fact the dissociated between Segment D of RNase E protein and Pnpase is in the μM range, which is not a strong interaction (Nurmohamed, Vaidialingam, Callaghan, & Luisi, 2009b). The "bridging" effect of RhlB could enhance the interaction between Pnpase and RNase E *in vivo.* Under physiological conditions, RhlB, and common substrate of RNase E and Pnpase, for instance, a long string of RNA could enhance such interactions drastically.

Building the RNA degradosome complex *in vitro* not only enables us to understand its function, but also makes it possible to investigate the role of RraA and RraB, which have been discussed in detail in Chapter 2. These two small proteins modulate the degradosome function *in vivo*, by specifically reducing the amount of RhlB bound upon over expression. Moreover, over expressed RraA and RraB generate distinct transcript profiles, suggesting that they utilize different strategies in modulating the degradosome complex and this effect to some degree is transcript-specific (Gao et al., 2006). To better undertand the mechanism of selective inhibition by RraA and RraB *in vitro,* we needed to produce high quality proteins that are devoid of ribonuclease and other contaminants for kinetic analyses. By expressing the protein in an RNase E truncation mutant strain, introducing denaturing purification step and following up with an ion exchange chromatography separation, such proteins could be generated at high purity and yield. In the next chapter I will describe the use of this *in vitro* reconstituted degradosome

complex in the presence of RraA or RraB to examine the effects of RraA/B on the *in vitro* hydrolysis of different RNA substrates.

CHAPTER 4 INHIBITION OF RRAA/RRAB ON RNASE E AND DEGRADOSOME

Introduction

In chapter 3 I described the reconstitution of RNA degradosome by individually purified degradosome components. In this manner, we can adjust the ratio of different components or add in the two protein inhibitors RraA and RraB in biochemical assays.

Because the Chapter 1 of this dissertation has summarized the structure, function and regulation of RNase E protein, the biochemical properties of RNass E which are of relevance to kinetic study, will be detailed in this introduction.

RNase E (E C 3.1.26.12) was first identified as 70KDa protein which can process 9S RNA in a stepwise manner. The 70KDa protein was later shown to be partially degraded RNase E since the full length protein is very unstable during purification (Mudd & Higgins, 1993). The cleavage of various RNA substrates of RNase E has been studied *in vivo* and *in vitro. In vivo* studies have relied on the use various RNase E mutants. Among these mutants, the best studied are *rne-1* and *rne3071*; the latter has amino acid substitutions in the S1 RNA binding domain of the N terminal Half of RNase E. These mutants confer temperature sensitive growth. Various C-terminal truncation mutants of RNase E have also been constructed, (e.g. *rne-131(Δ477), rneΔ610*) or isolated by exploiting the temperature sensitivity caused by defective for tRNA maturation. Current evidence supports the notion that the essentiality of RNase E is because of its role on tRNA processing (Ow & Kushner, 2002; Li & Deutscher, 2002; Söderbom, Svärd, & Kirsebom, 2005).

In vitro studies of the cleavage of, several well- defined short RNA substrates, such as BR10 and BR13(Redko et al., 2003) which are derived from the p23 RNA, long RNA substrates, such as RNA1 and 9S RNA, and various derivatives of 40 nucleotides long poly A RNAs by the N-terminal catalytic domain of RNase E have been performed. The specificity of RNase E has been studied by examining the effects of nucleotide

substitutions in the established RNA substrates listed above. A partial recognition motif for RNase E has been proposed from the cleavage of 27 nucleotides long RNA substrates: (G,A)(C,A)N(G)(GUA)_(A,U)(C,U)N(C,A)(C,A) (underline indicates RNase E cleave site) ((Kaberdin, 2003).

RNase E activity requires both monovalent ions e.g. Na^+, K^+, NH_4^+ and bivalent ions e.g. Mg^{2+}, Mn^{2+}. The optimum reaction pH is 7.6 to 8.0. The optimum reaction temperature is around 30 °C. RNase E can be irreversibly heat inactivated at 50°C (Misra & Apirion, 1979).

It has been reported that RNase E N terminal domain, as well as its bacteria homolog RNase G protein prefers a 5′ mono-phosphated than 5′ tri-phosphated RNA substrate. (Mackie, 1998; Jiang & Belasco, 2004) In this model, the naturally occurring 5′ tri-phosphated RNA transcript is a slow substrate for RNase E, however once it′s cleaved, a 5′ mono-phosphate is generated, and the rest of the transcript is degraded quickly, which is consistent with the “all or none” phenomenon in bacteria mRNA decay. Moreover, a 5′ pyrophosphatase activity has been discovered from *E.coli* recently, RNA pyrophosphohydrolase (RppH) removes the protective di-phosphate from the 5′ end of mRNA (Deana, Celesnik, & Belasco, 2008). However, the fact that *rppH* mutants selectively stabilize a set of transcripts suggests that 5′ end independent pathways exist in mRNA decay. Moreover, several mRNAs have been shown to be rapidly cleaved by RNase E independent of the phosphorylation status at their 5′ ends (Kime, Jourdan, Stead, Hidalgo-Sastre, & McDowall, 2009; Jourdan, Kime, & McDowall, 2010). Given

that most of the 5′ end-dependent substrates were either short single stranded RNA or long substrates that are being processed by RNase E near their 5′ extremities, it is tempting to hypothesize that the significance of the 5′ end in RNase E cleavage is dependent on whether the enzyme has "direct entry" into a single stranded site. This is supported by comparison of the structure of RNase E alone comparison to its RNA-bound form (Koslover et al., 2008b). Additionally the physiological significance of a 5′ mono-phosphate RNA substrate is not clear. An earlier *in vitro* study suggested that the consequence of a mono-phosphate over a tri-phosphate substrate is a faster catalytic rate, i.e. higher k_{cat} value (Jiang & Belasco, 2004). However a recent *in vivo* study suggested that the mono-phosphate binds to RNase E NTH with a higher affinity, i.e. a lower K_m value (Jourdan & McDowall, 2008). The protein structure data is in favor of the later notion (Koslover et al., 2008b).

Structural data and studies of the RNase E homologues indicate that the protein forms a tetramer (Callaghan et al., 2003; Zeller et al., 2007; Koslover et al., 2008b; Callaghan et al., 2005b) Whether this oligomerization affects its catalytic activity awaits more experimental elucidation. Truncation of the RNase E N-terminal half containing only the 1-395 residues which does not contain the domain interaction sites, thus assumed to be a monomer, remains kinetically active towards the BR30M RNA substrate, and is able to complement the *rne* null mutant (Caruthers, Feng, McKay, & Cohen, 2006). An earlier study using MBP-tagged RNase E NTH in which the MBP tag can prevent the tetramer formation, found that monomer RNase E cannot discriminate between 5′phosphate RNA

or 5′hydroxyl RNA, whereas the multi-metric state of RNase E cleaves the 5′ mono-phosphate substrate at least 18 times faster than the hydroxyl substrate. This indicates the requirement of tetramer formation in recognizing the 5′ mono-phosphate RNAs.(Jiang & Belasco, 2004)

Pnpase (EC 2.7.7.8) was first discovered in 1955 by Grunberg-Manago and Ochoa while studying phosphorylation in *Azotobacter vinelandii.* Initially the enzyme was considered as an RNA polymerase. Later it became clear that its main function in the cell is the reverse reaction, namely, phosphorylysis of RNA. Pnpase is an evolutionarily conserved enzyme found in all three kingdoms. In *E.coli* it is implicated in mRNA degradation and ribosome biogenesis. We have discussed the structure, regulation of *pnp* gene, and its interaction with RNase E and RhlB in detail in Chapter 1: Pnpase from *E.coli* consists of five domains, two RNase PH domains sited at the N terminals serve as catalytic core, and two RNA binding domains, KH and S1 located near the C terminal, with an all α helical domain linked in between. Pnpase catalyzes two different reactions under specific conditions: exchange of the β-phosphate group of nucleoside diphosphate and free orthophosphate; polymerization of single stranded RNA from nucleoside diphosphate and the reverse 3´ to 5´ processive phosphorylysis of RNA, releasing nucleoside diphosphate. As aforementioned, the processive phosphorylysis reaction is inhibited by low inorganic phosphate concentration or high ATP concentrations (Del Favero et al., 2008). Pnpase requires a single-strand region near the 3′ of RNA for phosphorylytic degradation of RNA. A minimal of 7-10 nucleotides 3´ overhang enables specific substrate binding to

Pnpase. *In vivo,* this requirement is met by two means: addition of poly (A) tails or by RhlB unwinding. Pnpase can exist as $\alpha_3\beta_2$ complex where the β subunit is RhlB. This interaction between Pnpase and RhlB is independent of RNase E.

The optimal pH for Pnpase phosphorylysis reaction is between 8 and 9.5. The preferred divalent mental for Pnpase is Mg^{2+} or Mn^{2+}. For oligonucleotides (between 2-10 nucleotides) the K_m for phosphate is 0.7mM, which is independent of substrate sequence. The K_m for oligonucleotides ranges from 0.13mM (4nt) to 0.05mM (6nt and higher). The trend is that within a series of oligonucleotides containing similar sequences, the K_m decreases as the chain length increases, eventually reaches a plateau at a concentration of 50μM for the *E.coli* Pnpase. In the case of polynucleotides longer than 20 nucleotides, the K_m keeps decreasing with length and reaches the nM range for substrates longer than 100 nucleotides (Godefroy-Colburn, T.; Grunenberg-Manago, 1972). The change in K_m values according to substrate length indicates multiple RNA interaction sites on Pnpase. Indeed, the phosphorylysis of polynucleotide is "processive", i.e. Pnpase binds to the substrate, degrades the entire substrate to completion prior to binding and degradation of another polynucleotide. It is worth mentioning that the phosphorylysis of short oligonucleotides by Pnpase occurs in a non-processive manner. Moreover, it has been hypothesized RNAs trapped in certain conformations are resistant to Pnpase degradation, e.g. certain tRNA species *in vivo* are resistant to Pnpase degradation (Littauer, U.Z.; Soreq, 1982).

Pnpase has been identified as a cold shock protein. Pnpase deletion mutant cannot grow at lower than normal temperatures. The knowledge about Pnpase function in the cold is still rudimentary. Certain mutations in the KH and S1 domains confer cold-sensitivity. A truncated form of Pnpase lacking the S1 domain was able to complement the cold sensitivity of a *pnp* deficient nonsense mutant. This domain located in the C-terminal region of Pnpase is believed to contribute to its processivity. Mutations in this region, although have limited effect on phosphorylysis activity, significantly affect substrate binding and thereby increase the K_m (Briani et al., 2007).

Compared with RNase E and Pnpase, the role of RhlB is not well understood at the molecular level. RhlB belongs to a protein family named DEAD-box RNA helicase. Besides the structure organization and some functional properties discussed in Chapter 1, here I focus on its specificity, kinetic properties and mutagenesis of RhlB.

To date, there are five DEAD-box RNA helicases known in *E.coli:* DbpA, CsdA, RhlE, SrmB and RhlB. Only one of these five enzymes, DbpA, displays sequence-specific substrate binding, and is involved in 23S rRNA processing. The other four DEAD-box RNA helicases may require interaction with other proteins for sequence recognition. Of particular interest to this study, RhlB is known to interact with the C terminal fragment of RNase E and Pnpase separately.

DbpA unwinding requires single-strand extensions at the 3´ extremity of an RNA duplex. Such single-strandness requirement is not rigid in the other four helicases involved in RNA processing. This is probably also due to the availability of protein partners which

present them the substrate. CsdA and SrmB can utilize either 3´ or 5´ extensions, whereas RhlE can unwind duplexes with blunt ends (Iost & Dreyfus, 2006). RhlB, in contrast to the other four DEAD-box helicases, do not process unwinding activity or ATPase activity on its own *in vitro.* ATP hydrolysis and RNA unwinding is detected when RhlB is activated by a peptide fragment from the C-terminal of RNase E (628-843aa).Because this region of RNase E is implicated in RNA binding, the observed 5′ single-strandness requirement in the RNA unwinding assays by RhlB/RNE (628-843aa) complex (Iost & Dreyfus, 2006) could be a consequence of the RNase E fragment it binds to.

RhlB, like most DEAD-box RNA helicases involved in RNA processing, has very poor processivity. Therefore *in vitro* assays for RhlB and other DEAD box enzymes unwinding activity are performed either by using an excess amount of enzyme relative to substrate, or in a coupled reaction whereby the unwound RNA is immediately degraded by other ribonucleases. Recently, Cartier *et al.* developed a continuous helicase assay using a FRET RNA duplex in the presence of large excess of unlabeled complementary RNA oligos (Cartier, Lorieux, Allemand, Dreyfus, & Bizebard, 2010). In this assay it is assumed that the presence of excess RNA oligos do not affect substrate binding to the helicase during the measured reaction time. However this method is still unable to derive K_m values for the RNA substrate. Using this assay K_m values for ATP hydrolysis was calculated to be within the milimolar range for RhlE and less than 100μM for SmrB. In agreement with the poor processivity of the DEAD box helicases, the unwinding rate

constants decrease drastically when the length of the duplex increases from 9 base pairs to 11 base pairs for both SmrB and RhlE.

CsdA is associated with degradosome after cold shock or when RraB, the RNase E inhibitor is over expressed. It′s worth mentioning that, CsdA binds at a different site on RNase E than RhlB i.e. their binding is not mutually exclusive. Although three of the five DEAD-box RNA helicases have been implicated in cold adaption, a mutant devoid of RhlB does not show such a phenotype.

There are several RhlB mutants that have been generated by site direct mutagenesis based on rational design. The active site mutant RhlB H320D loses ATPase activity in the presence of RNase E fragment (696-762aa), even though it still binds to the RNase E fragment avidly and forms a proper structured protein complex. F10A is a mutation in the RNA binding region of RhlB. This mutant was shown to form a complex with RNase E (696-762) and showed significant ATPase activity without RNA, but surprisingly little activity when RNA was present. Another mutant, F10M, when bind to an RNase E fragment, also had little activity when RNA was present, but its activity without RNA was comparable to wild type RhlB/RNase E fragment complex when RNA was present. In other words, the F10M mutation mimics the situation where RNA activates the ATPase activity in wild type enzyme, however when RNA is present, such an "activation" state is disturbed by RNA binding (Worrall, Howe, McKay, Robinson, & Luisi, 2008).

The existence of enolase in the RNA degradosome is mysterious. As a glycolytic enzyme, enolase has been the subject of systematic studies of its structure, function and kinetic properties (Reed, Poyner, Larsen, Wedekind, & Rayment, 1996). However, how enolase affects mRNA turnover by RNA degradosome is unknown.

Using the degradosome complex reconstituted *in vitro* as described in Chapter 3, in this chapter, I tested the consequences of RraA and RraB binding on the kinetics of RNA degradation: First, the effects of RraA and RraB on RNase E hydrolysis of a 14 nucleotide synthetic RNA substrate were determined. Second, the effect of RraA and RraB on the cleavage of two different polynucleotides RNA substrates with different tertiary structures was also investigated. A moderate degree of mixed inhibition was observed for both RraA and RraB on the hydrolysis of the 14 nucleotide synthetic RNA substrate. By comparison, the processing of a long RNA namely the *dsbC* mRNA by RNA degradosome is severely inhibited by RraA or RraB.

Materials and Methods

RNase E activity assays using FRET RNA substrates

The P-BR14-FD fluorogenic RNA substrate was synthesized and HPLC-purified by TriLink (San Diego, CA). The kinetic assays were performed in reaction buffer (25mM bis-Tris propane (pH 8.0), 100mM NaCl, 15mM MgCl2 and 1mM DTT). No background RNase activity (i.e. increase in fluorescence signal) was detected using this buffer. The concentrations of proteins in each reaction were RNase E (tetramer) 0.25μM, BSA or

RraA/B (monomer) 2.5μM. The proteins were incubated on ice for 10 minutes first, then warmed to the reaction temperature prior to use. The FRET substrate (final concentration varied from 2.5 to 12.5μM) was added, and the reaction was carried out at 25ºC on 96 well plates, and the change of fluorescence signal was measured on a Synergy HT fluorescent plate reader (BioTek, VT) with a 485/20 excitation filter and a 516/20 emission filter. The initial rate of each reaction was determined as the slope from the linear kinetics under different substrate concentrations. The initial rates and derived K_m and V_{max} were calculated using Kaleidagraph v3.6 (Synergy, PA).

DEGRADOSOME ACTIVITY ASSAY

To examine the effects of RraA/RraB on the activity of RNase E-RhlB complex, RNA1 and *dsbC* was used as substrate, and the loss of the full length RNA band were monitored by gel electrophoresis. Reactions were carried out at 37ºC in reaction buffer (1mM ATP, 1mM DTT, 1mM MgCl2, 25mM Tris-HCl pH8.0 in 1x PBS). The buffer was made by diluting RNase-Free buffer sets purchased from Ambion. RNase-Free PCR plates were used to perform the assay on Applied Biosystem 2720 Thermal Cycler. RraA/B proteins were incubated with degradosome proteins on ice for 30mins prior to the reaction. RNA substrates were diluted in reaction buffer and refolded by incubating at 70ºC for 10mins first then the temperature was gradually decreased to 30ºC over 40mins. The refolded RNA and incubated proteins were then combined together to start the reaction at 37ºC. At each time point, 5μl of properly diluted proteinase K (NEB) was added to the tube to stop the reaction. The amount of proteinase K added was adjusted to the amount of protein in

the reaction tube. After 30 minutes of digestion by proteinase K at 37ºC, the enzyme was inactivated by heating at 75 ºC for 15 mins. 10ul of the 30ul reaction mixture were mixed with 2x gel loading dye and the samples were analyzed on 10% Criterion TBE-Urea Gel (BioRad, CA). After electrophoresis, gels were stained with SYBR Gold stain (Invitrogen, CA) and visualized using Typhoon 9400 scanner. The band intensity was quantified by Image Quant.

IN VITRO TRANSCRIPTION OF RNA SUBSTRATES

DsbC mRNA truncation template was PCR amplified from plasmid pET28a-DsbC using primers covering the T7 promoter region to the 250th nucleotide of the *dsbC* ORF. The RNA1 template was difficult to PCR amplify due to its complicated secondary structures, we used a restriction digested fragment from a plasmid (pIDTSMART-T7RNA1) containing the T7 RNA polymerase promoter site followed by the RNA1 sequences. The plasmid was purified by Maxi prep (Qiagen, CA), digested with EcoR1 and gel-purified to generate linear dsDNA template for in vitro transcription using Megashortscript™ Kit (Ambion, TX). Transcripts were purified with MEGAclear Kit (Ambion, TX), RNA was properly diluted and quantified by Nanodrop® ND-1000A, following the equation C (μg/mL) $\approx$ 33 x A_{260}.

QUANTITATIVE REAL-TIME RT-PCR

RNA was reverse transcribed into cDNA using a gene-specific primer (5′-AAC AAA AAA ACC ACC GC-3′, complementary to 17 bases of RNA1 at the 3′ end) and

SuperScript III Reverse Transcriptase (Invitrogen, CA) according to the manufacturer′s instructions. For detection and quantification of the uncleaved RNA1, the ABI PRISM 7900HT Sequence Detection System was used. Real-time PCR reactions were performed with goTaq® qPCR master mix (Promega, WI) according to manufacturer′s protocol. The specificity of the reaction products was confirmed by dissociation curve analysis. Each sample was tested in triplicate, and the change in RNA1 levels was calculated using the $\Delta\Delta C_t$ method and normalized by a reference DNA. Primer pairs for Real time PCR were designed based on SciTools on the idtdna website.

QUANTITATIVE ANALYSIS OF INHIBITION PERCENTAGE

Reaction rates in the presence or absence of various amounts of inhibitors, as measured by either fluorescence assays or the real time PCR was plotted as relative activity (percentage activity) over the concentration of inhibitor. The data were plotted and fitted to the equation shown below using the non-linear regression of Kaleidagraph:

$$activity\% = (100 - activity\%_{min}) * e^{(-k*[inhibitor])} + activity\%_{min}$$

$$inhibition\% = (100 - activity\%_{min})$$

Results

MICHAELIS-MENTEN PARAMETERS FOR THE RNASE E HYDROLYSIS OF FRET OLIGONUCLEOTIDES

A fluorescence resonance energy transfer (FRET) modified 14mer RNA substrate originally described by Jiang (Jiang & Belasco, 2004) was used in this study to derive the Michealis-Menten parameters for the hydrolysis of short RNAs by truncated RNase E lacking the C-terminal 16 amino acids. This FRET fluorogenic RNA substrate, P-BR14-FD, resembles the 5′ terminal of pBR322 RNA1 which contains a single major RNase E cleavage site. The substrate RNA is designed in a way that there is a fluorescein tag upstream of the expected RNase E cleavage site and a fluorescence-quenching dancyl tag downstream of the cleavage site. Cleavage by RNase E results in a marked increase in fluorescence. Alternatively, cleavage can be determined by gel electrophoresis based on the different sizes of substrate and product.

Although the crystal structure demonstrated that the N terminal catalytic domain of RNase E can accommodate a 14 nucleotide RNA, little is known about the effects of the RNA binding site which is located at the central region of RNase E (and is not present in the N-terminal catalytic fragment used for earlier studies) to its catalytic activity. To this end, we used the RNase E fragment (RNase E1045) lacking only 16 amino acids at the very end of C-terminal for kinetic assay, and compared the kinetic parameters with the ones obtained previously using NTH RNase E. The K_m value obtained with RNase E

1045 was 5-fold higher than that for RNase E498 which contains 1-498 residues of RNase E (3.2μM versus 0.6μM). This might be due to the presence of the additional binding site provided by the central region of RNase E, which competes for the substrate with the RNA binding site within the catalytic core. The k_{cat} value obtained with RNase E 1045 is similar to that for RNase E 498, within 1 min^{-1} range. (Figure 4.1)

A

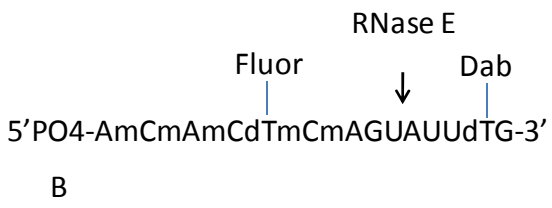

B

Proteins	K_mμM)	k_{cat}(min^{-1})	k_{cat}/K_m
0.25μM RNase E +2.5μM BSA	3.2±0.4	0.99±0.03	0.31±0.04
0.25μM RNase E +2.5μM RraA	4.4±0.4	0.87±0.03	0.20±0.02
0.25μM RNase E +2.5μM RraB	5.6±0.8	0.85±0.05	0.15±0.02

C

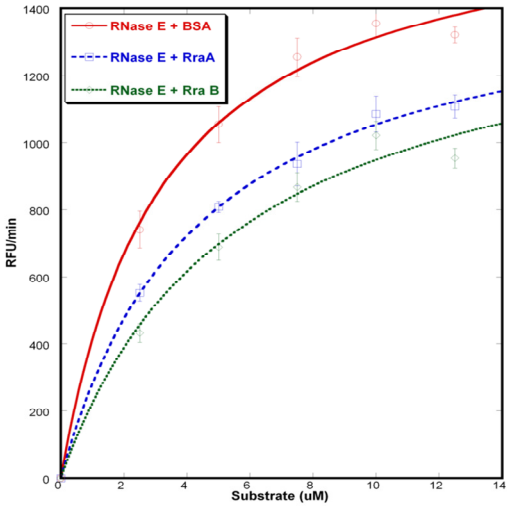

Figure 4.1 Michaelis-Menten parameters for the hydrolysis of FRET substrates. A. The FRET substrate used in kinetics assays. The cleavage of RNase E as indicated by the arrow separates the fluorophore from the quencher and results in more than 30 fold increase in fluorescence signal. (Adopted from Jiang et al. 2004). B. Michaelis-Menten parameters derived from steady state analysis using 0-12.5μM FRET RNA substrate (shown in C). Quadruplicate data were analyzed using KaleidaGraph. RNase E was incubated with RraB (green) RraA (Blue) or BSA (red) on ice for 10 minutes before FRET RNA was added and the reaction starts. The initial rate of each reaction was determined as the slope from the linear kinetics under different substrate concentrations.

INHIBITION OF RRAA AND RRAB TO RNASE E HYDROLYSIS OF FRET OLIGONUCLEOTIEDS

RraA and RraB bind to RNase E at the 628-843aa and 694-727aa regions, respectively, both of which are away from the RNase E catalytic core implicated in RNA binding. One

would expect that the mode of action of these inhibitors would fit neither competitive inhibition nor noncompetitive inhibition. Indeed, our data suggest that RraA and RraB both have only moderate effects on K_m and k_{cat} of RNase E in the FRET substrate hydrolysis and display a mixed inhibition pattern (Figure 4.1). Interestingly, the inhibition by RraB is more severe than that by RraA, as judged by the k_{cat} /K_m values. However, when plotting the inhibited activity (percentage activity) over inhibitor concentration, as shown in Figure 4.2, the maxium amount of inhibition, as calculated by an exponential fit, is 60% for RraA versus 44% for RraB under the conditions described.

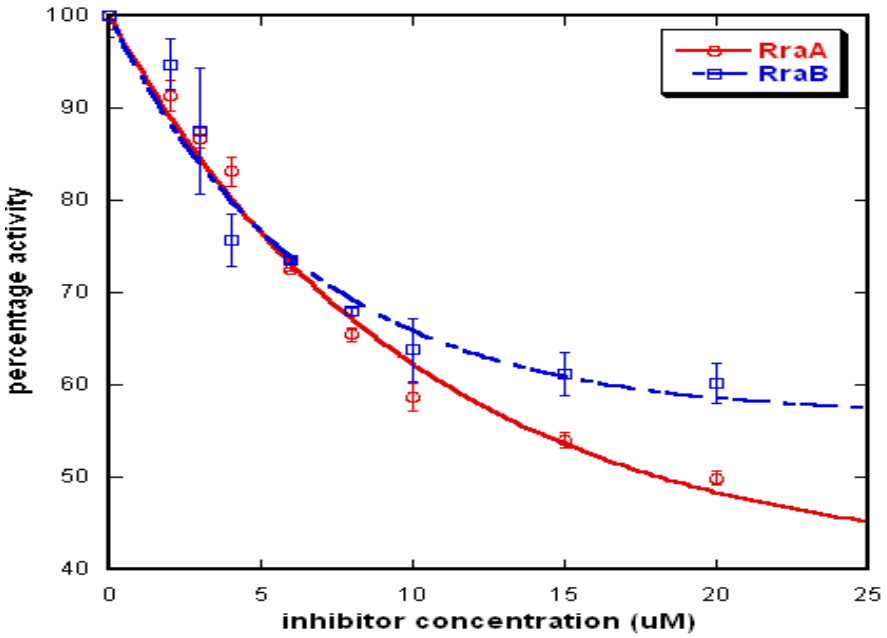

Figure 4.2 Inhibition by RraA/B of 1μM (monomer) RNase E in the hydrolysis of 5 μM FRET RNA substrate. Exponential base e curve fit was used to plot activity change over inhibitor concentration (μM of monomer).

DEGRADATION OF LONG RNA TRANSCRIPTS BY THE DEGRADOSOME *IN VITRO*.

Very little is known about how RNase E cleaves RNA substrates in presence of other components of the RNA degradosome. With our RNase E 1045 fragment, which includes not only the N-terminal catalytic half but also the binding sites for RraA/RraB, RhlB and enolase, we were able to evaluate the effect of these factors.

Earlier *in vivo* microarray studies suggested that mRNA degradation requires the coordination between different degradosome components. (Bernstein, Lin, Cohen, & Lin-Chao, 2004) To test the inhibitory effect of RraA/RraB under such circumstances a system was developed to reconstitute a minimal degradosome in vitro and examine the effects of RraA/RraB on the complex against different substrates. For these assays I adopted a more physiologically relevant RNA substrate, i.e. a truncated *dsbC* mRNA which is 300 nucleotides in length.

Earlier studies by our lab established that *dsbC* mRNA processing involves RNase E. *In vivo*, lesions in *rne* increase the half life of *dsbC* mRNA from 0.82min to about 2mins. (Zhan et al., 2004) Moreover, RraA and RraB were first discovered as inhibitors of mRNA degradation based on a genetic search for genes that increase DsbC activity. When RraA or RraB is over expressed in the cell, the half-life of *dsbC* mRNA is three to five-fold longer (Gao et al., 2006). Gao *et al.* used a probe hybridizing to the first 1-266 nucleotides of the *dsbC* transcript.(Gao et al., 2006). Here I used *in vitro* transcribed truncated version of *dsbC* mRNA including a short region of the *lac* operator (from the plasmid vector it is transcribed from) and the 1-250 nucleotide of *dsbC*.

The degradation of this RNA requires the cooperative action of RNase E and RhlB, which is consistent with the Mfold structure prediction indicating that the *dsbC* mRNA forms multiple stem-loop hairpin structures within the first 250 nucleotides. As shown in figure 4.3, RNase E alone cannot degrade this transcript. In the presence of RhlB, the 300nt RNA was degraded within 30mins under the reaction conditions we applied. Interestingly, when Pnpase was added into the system, forming an RNase E-RhlB-Pnpase partial degradosome, the substrate persisted for up to 75mins. Surprisingly, a reaction intermediate of about 200 nucleotides long was observed in reactions containing Pnpase but not in its absence, one possible explanation is that this RNA is trapped in a conformation that is being protected by Pnpase from further degradation. Intriguingly, addition of enolase accelerated the reaction compared to the partial degradosome complex without enolase.

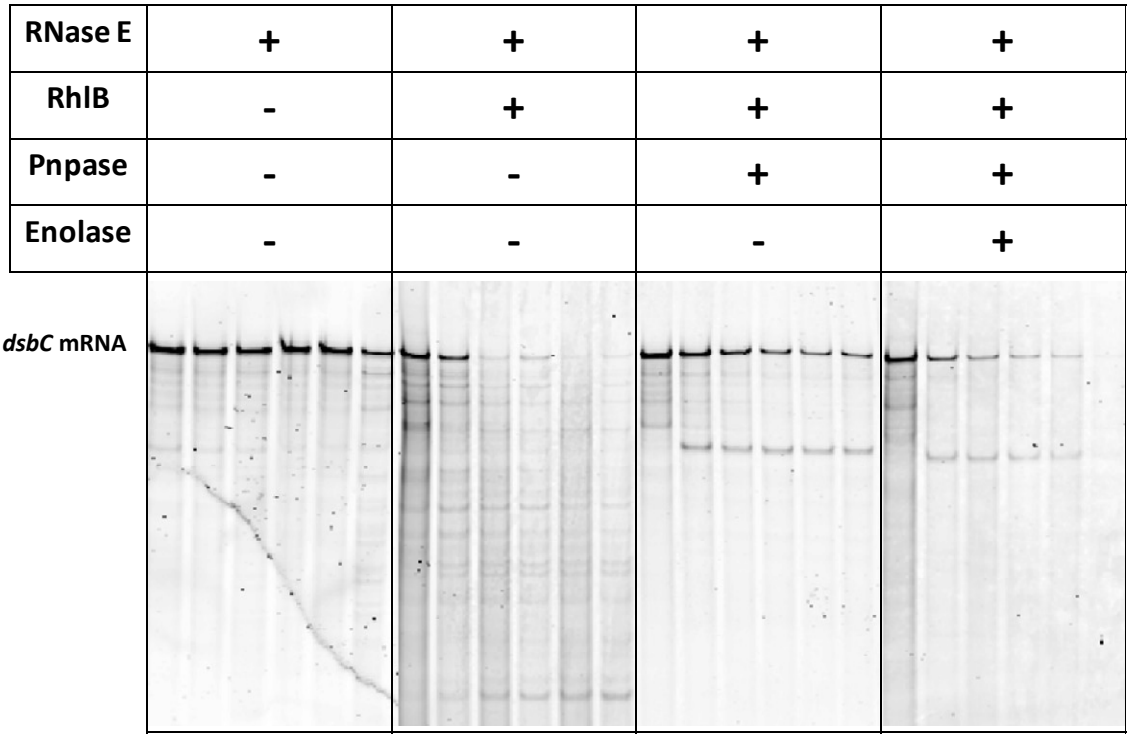

Figure 4.3 Degradation of *dsbC* mRNA. The assay was done under the conditions described in Materials and Method. The amount of RNA and proteins used in each reaction (monomer concentration) 25nM *dsbC* mRNA, 5nM RNase E, 80nM RhlB, 30nM Pnpase, and 40nM Enolase.Samples was taken at various time points: 0, 15, 30, 45, 60 and 75mins.

Compared to *dsbC* mRNA, RNA1 has a longer half life *in vivo* (0.82min *versus* more than 3min). The degradation of RNA1 also requires RhlB unwinding activity. The involvement of Pnpase in RNA1 degradation requires the addition of a poly A tail, the effect of enolase on RNA1 degradation is still under investigation.

INHIBITION THE RNA DEGRADOSOME BY RRAA AND RRAB

It was reported that the K_i value for the inhibition of the BR13 substrate by RraA is 2.5μM. Under similar conditions the K_i value for the pM1 RNA substrate degradation by RNase E was reported as 0.5 μM (Lee et al., 2003). In the case of *dsbC* mRNA, RNase E protein alone cannot degrade this 300 nucleotides long transcript on its own efficiently, and other degradosome components, especially RhlB are required for the fast degradation of RNA. We explored the inhibitory effect of RraA or RraB on the inibhition of degradosome activity. We showed in Figure 4.4 that 0.12 μM of either inhibitor successfully inhibited the reaction to more than 50%. Due to the limitations of the dynamic range in gel electrophoresis, we could not perform systematic kinetic assays to calculate K_i values. This data demonstrated that nanomoler concentrations of RraA or RraB, which is comparable to substrate concentration applied in the assay, can cause drastic stabilization of transcripts susceptible to degradation by the degradosome complex.

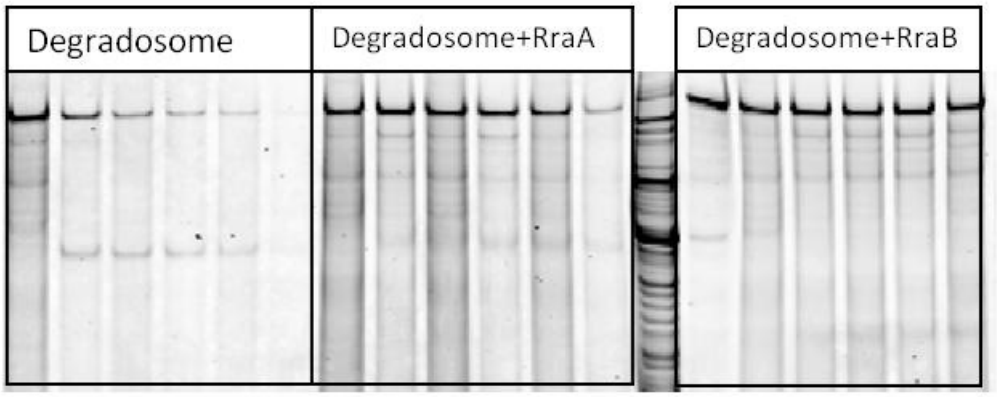

Figure 4.4. Inhibiton of RraA and RraB on the degradation of *dsbC* mRNA. Reaction conditions were same as Figure 4.3, except that 120nM of RraA or RraB were added in

the reaction as indicated in the panels on top. Reaction time: 0, 15, 30, 45, 60, and 75mins.

RNA1 is a small regulatory RNA used by ColE1 origin plasmid to control its copy number. It affects the plasmid copy number by binding and thus inhibiting the maturation of RNAII which serves as the DNA replication primer once it is processed. RNA1 is a short RNA transcript slightly longer than 100 nucleotides in length which folds into a cloverleaf structure. The central loop of this cloverleaf is important for base-pairing with its target RNAII. It was also suggested that this interaction does not involve a large number of bases (Lacatena & Cesareni, 1981). The sequence specific RNA1-RNAII interaction is enhanced by a 63 amino acids small protein encoded by the plasmid, Rom (RNA one modulator). Rom recognizes either the complex formed by two RNAs and stabilizes it or the individual RNAs and induces a stable complex formation. It is interesting that Rom stabilized a specific RNA conformation irrespective of its exact sequence (Eguchi & Tomizawa, 1991). The structure of the loop-loop complex formed between the RNA1 and RNAII complementary loops has been solved. Although the 7 nucleotides that are involved in this interaction form a perfect Watson-crick base pair, the structure of the complex is different from the A form of RNA helices. Instead, the loop-loop complex bends towards the major groove, thereby narrowing it. This bending feature is proposed to be the sequence-independent structure feature that is recognized by the Rom protein (Lee & Crothers, 1998). RNase E is involved in degradation of RNA1. The degradation of RNA1 by RNase E has been studied *in vivo* and *in vitro* (Bouvet &

Belasco, 1992; Kaberdin, Chao, & Lin-Chao, 1996). The half life of RNA1 is about 3 minutes in wild-type E.coli strains. The degradation of RNA1 is triggered by RNase E cleavage at a unique site near the 5´ end, and this endonucleolytic cleave is sensitive to the 5´-terminal base paring (Bouvet & Belasco, 1992). Besides the initial attack by RNase E at the 5´ terminal of RNA1, multiple cleavage sites located in the bubbling regions of its stem loops has been identified *in vitro* (Kaberdin, Chao, & Lin-Chao, 1996). Using various *rne* deletion mutants, the degradation pathway of RNA1 has been studied in detail. It was shown that the ARRBD region of RNase E is essential for the initial endoribonucleolytic cleavage of RNA1, which indicates the involvement of RhlB in unwinding the secondary structure of RNA1 (Nishio & Itoh, 2009). In recent studies of RraA and RraB, the copy number of the ColE1 origin plasmid was used as an indicator of RNase E activity *in vivo* (Lee, Yeom, Sim, Ahn, & Lee, 2009; Yeom et al., 2008). It is noteworthy that another RNase E inhibitor, L4, also has stabilizing effect on the RNA1 transcript *in vivo* (Singh et al., 2009).

We showed that RNase E alone poorly process RNA1 *in vitro* (data not shown) and that the reaction is greatly accelerated by addition of RhlB, presumable because of its RNA unwinding activity. Our data (Figure 4.5) suggested that under the reaction conditions used here (i.e. RNase E-RhlB partial degradosome) RraB inhibits the decay of RNA1 to a greater extent relative to RraA. This is consistent with the findings *in vivo* as mentioned above where over expression of RraB causes a greater reduction in ColE1 origin plasimid copy number (Yeom et al., 2008). Based on the decrease in band intensity of 105

nucleotides long RNA1, which is the product formed after first 5 nucleotides has been processed, the gel showed in Figure 4.5 suggested that under the conditions used, RraA reduced the reaction rate by 40% whereas RraB reduced the reaction rate by more than 50%.

Real time PCR analysis was used to quantify various amount of full length RNA1 remaining at different time points. The primers used for the Real time PCR were designed in a way that only full length RNA1 could be amplified, which means we specifically monitored the fast cleavage reaction happening at the first 5 nucleotide site. We used Real time PCR to monitor the loss of full length RNA1 because the band intensity of this full length RNA could not be quantified at low substrate concentrations. The detection limit of Real time PCR method was much lower and suitable for such analysis. Our data showed that RraA inhibited the fast cleavage reaction by approximately 35%, whereas RraB inhibited the reaction by about 80% as shown in Figure 4.6 (exponential fit). A 400 base pair double stranded PCR product unrelated to RNA1 was used for both the gel electrophoresis assay and for real time PCR assays as a loading (internal) control.

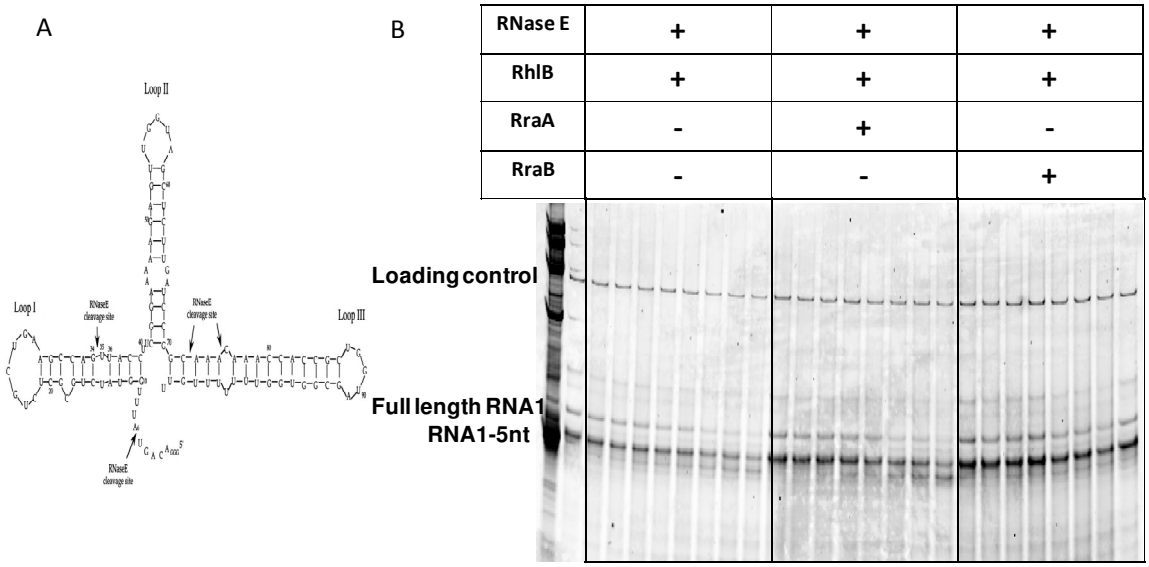

Figure 4.5 Inhibition on the decay of RNA1. A.The secondary structure of RNA1 and multiple RNase E cleavage sites on it (Kaberdin, Chao, & Lin-Chao, 1996). B. Degradation of RNA1 by RNase E and RhlB partial degradosome and inhibition by RraA and RraB. The RNA and proteins used in the reactions were: 24nM RNA1, 5nM RNase E, 80nM RhlB, 120nM RraA or RraB. Reaction time: 0,15,30,45,60,80,100 and 120mins.

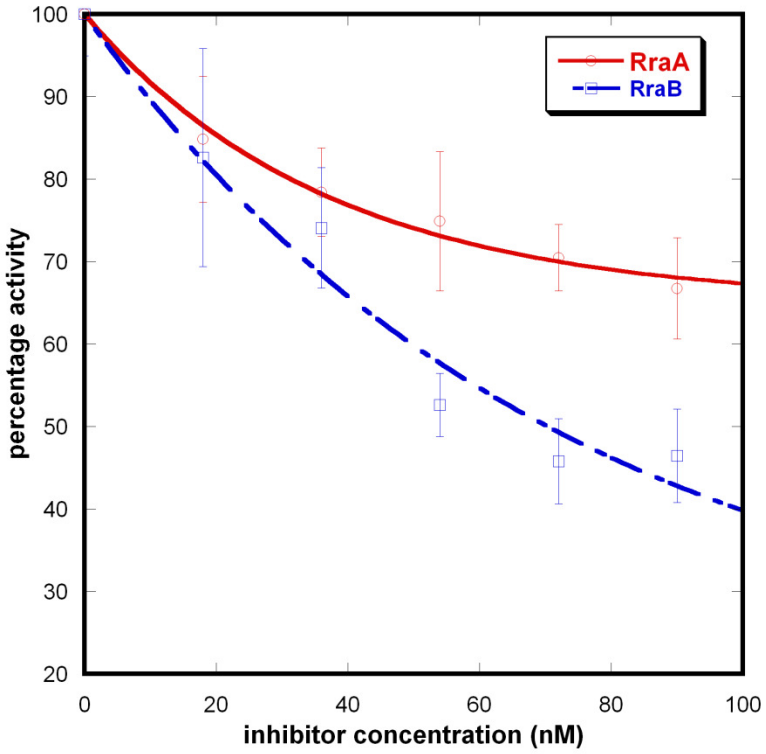

Figure 4.6 Inhibition of RraA/RraB on 5nM RNase E and 80nM RhlB processing of 24 nM full length RNA1, as measured by Real time PCR. Relative reaction rates were derived from the average of triplicates data. An exponential base e curve fit was used to plot activity change over a gradient of inhibitor concentration. All protein concentrations were demonstrated as monomer concentration.

Discussion

Although the N-terminal catalytic half of RNase E has been used in numerous kinetic studies using various RNA substrates, little is known regarding the role of the central and C-terminal region in RNA processing. As the first and preliminary step of investigating RraA/RraB inhibition, we purified the 1045 amino acids truncated version of RNase E,

and compared its catalytic properties to its N-terminal half portion (1-498 aa). Our data indicated that the catalytic activity k_{cat} is comparable for both versions of RNase E truncation. However, the K_m for the synthetic FRET RNA is increased in RNase E 1045, which may due to the competitive binding between two different RNA binding sites, one in the catalytic domain and other near the central region. It was recently reported that RNase E hydrolysis of short RNA substrates displayed two phase kinetics (a boost at the first 10 mins then a slow steady phase that lasted for hours) (Jourdan, Kime, & McDowall, 2010). We also observed a similar phenomenon. In our analysis we calculated the steady state kinetics parameters for the second, slow phase. The kinetics of the slow phase were similar to those published earlier for the N-terminal half of RNase E (Jiang & Belasco, 2004).

The discovery of RraA and RraB revealed a novel regulatory mechanism whereby the remodeling of the RNA degradosome affected the half life of mRNA and thus the abundance of the respective proteins (Kangseok Lee 2003). In this chapter, we showed that RraA and RraB moderately inhibit RNase E hydrolysis of the 14 nucleotide synthetic RNA in a mixed inhibition manner. Furthermore, inhibiton was saturated at stoichimetric ratios of RraA/RraB, where approximately 50% inhibition is reached.

Over expression of RraA/RraB alters the composition of RNA degradosome *in vivo* (Gao et al., 2006). To test the effect of the inhibitors on RNA processing by the RNA degradosome, RNase E, RhlB, enolase and Pnpase were purified individually and allowed to a complex *in vitro*. The presence of RraA/RraB resulted in significant

inhibition of the degradosome in the decay of *dsbC* mRNA, whereas moderate inhibition were found for degradation of RNA1.

During our analysis of RNA1 degradation, we realized the limitations of gel electrophoresis assay especially their low sensitivity. By designing proper primer pairs we developed a Real time PCR which provided greatly increased sensitivity. We speculate that this method will be very useful in future for two reasons: first its high sensitivity and relative high throughput will reduce the amount of effort required for conventional RNA assays using gel electrophoresis; Second, by designing the suitable primers, various intermediates during RNA decay pathway can be specifically quantified simultaneously, making it possible to dissect the fast and slow steps of RNA decay pathway.

How do RraA and RraB inhibit RNA decay? Based on the work presented here, we propose that RraA and RraB can reduce the intrinsic activity of RNase E and carry out their inhibitory function mostly by interfering with the coordination between different RNA degradosome components in vivo. The significant inhibition we observed for the cleavage of the *dsbC* mRNA, relative to the moderate inhibition of the FRET substrate hydrolysis supports this hypothesis. Moreover, a recent paper demonstrated that RraA affects RNA binding by RhlB-RNase E complex *in vitro* (Gorna et al., 2010). A quantitative way of testing this hypothesis is compare the composition of *in vitro* reconstituted degradosome complex in the presence and absence of RraA/RraB inhibitors. Moreover, the effect of addition of inhibitor proteins on the affinity between

RNase E and RhlB, or RNase E and enolase can be directed measured and compared. These *in vitro* experiments will also clarify whether the previous observed RraA/RraB over expression induced degradosome composition change *in vivo* is a direct effect of the inhibitor protein.

CHAPTER 5 CONCLUSIONS AND RECOMMENDATIONS

This work sought to shed light on the roles and mechanisms of action of RraA and RraB, two small protein inhibitors of RNase E. The transcriptional regulation of *rraA* was investigated. Microarray data had suggested that the *rraA* mRNA level increases upon entry into stationary phase. We found that *rraA* is transcribed from its own protomer P_{rraA}, located in the intergenic region between *rraA* and *menA*. The promoter P_{rraA} was shown to be *rpoS* dependent (Zhao, Zhou, Kawarasaki, & Georgiou, 2006).

The transcription of the *rraB* gene was shown to be more complicated. Like *rraA, rraB* is transcribed by its own promoter P_{rraB} located in the intergenic region between *rraB (yjgD)* and *argI.* Although the expression of the *rraB* gene was to be repressed under tryptophan starvation conditions (Khodursky et al., 2000), we found no evidence that the promoter activity of P_{rraB} *is sensitive* to the availability of tryptophan. Similarly, arginine availability does not affect the P_{rraB} promoter activity either, even though the gene encoding the Arg repressor protein ArgI overalps P_{rraB} in E.coli and this genomic organization is conserved in several species of proteobacteria. To explore the physiological significance of *rraB,* transposon mutagenesis followed by screening for higher LacZ activity from a P_{rraB}*::lacZ* transcriptional fusion was employed. A transposon mutant library was generated, and more than 30, 000 colonies were screened based on LacZ activity as monitored by blue-white screening. A transposon insertion that occurred near the central region of the *glmS* gene resulted in elevated expression of *lacZ* from the P_{rraB} promoter. This was further confirmed with complementary assays

examining the effect of Glucosamine-6-Phosphate, the end-product of the enzyme GlcN-6-P synthase. The mechanism by which reduced activity of GlmS affects RraB expression awaits further investigation.

In vitro RraA and RraB were demonstrated to exhibit a moderate inhibitory effect on RNase E hydrolysis of a 14mer FRET RNA substrate. We showed that the RNase E 1045 resulted in a higher K_m compared to a fragment comprising of only the catalytic domain (1-498aa). One possible explanation for this observation is that there is competition for RNA binding among the RNA binding motifs located within the catalytic core and the central region of RNase E. Degradation of long, structured RNA such as RNA1 and *dsbC* mRNA requires the coordination of activities between RNase E and RhlB. Because the binding sites of RraA and RraB overlap with the RhlB binding site on RNase E, it is reasonable to postulate that the inhibitory effect might result from displacement or interference with RhlB activity However, we also observed that the cleavage of the *dsbC* mRNA was inhibited much more strongly than that of RNA1 indicating that the presence of RraA affects other factors in RNA turnover in addition to RhlB. Of note, our study of the RNA degradosome is the first reconstitution analysis of this RNA processing machinery by adding back the RNA degradosome component one by one.

Recommendations

We have demonstrated in this work how RraA and RraB inhibit RNA processing by the RNA degradosome. However, the effect of the inhibitor proteins on the degradosome composition had not been investigated. Size exclusive chromatography, co-immuno precipitation or sedimentation analysis can be employed to evaluate the molecular weight of degradosome in the presence of different molar ratios of RraA/RraB. An *rraA*$^-$ *rraB*$^-$ double mutatnt is viable and does not display significant growth defects indicating that *E.coli* may encode additional Rnase E inhibitors. One way to identify genes encoding such proteins would be to search for synthetic lethal alleles. A convenient synthetic lethality screen is now available (Bernhardt & de Boer, 2004). Briefly, a copy of wild type *rraA* gene is carried on an F plasmid, as well as a downstream reporter *lacZ* and the plasmid is transformed into a host devoid of *rraA*. Formation of a colony with a blue center and white edges on LB agar plate is the result from the loss of F plasmid (which is unstable in a particular genetic background) during replication. However, when a gene X (unknown gene) which is required for supplementing *rraA* function is disrupted by mutagenesis of *rraA*- strain, the loss of F plasmid would be lethal under such circumstances thereby forming solid blue colonies that retain the F plasmid. In this way, we expect discover more RNase E modulators, or additional physiological functions of RraA. However it should be noted that a preliminary search for synthetic lethal alleles was not successful (data not shown).

RNA1 plays a significant role in control of ColE1 origin plasmid replication, and its degradation by RNase E is well established. In wild type *E.coli* strains, the half life of RNA1 is about 3 mins. An engineered RNA1 which is less susceptible to RNase E degradation, yet functionally active, *i.e.* forms a complex with RNAII and inhibits plasmid replication could be useful in fine tuning the plasmid copy number at will. Putting such RNA under a controlled promoter could add another layer of plasmid copy number control and can be advantageous in downstream applications.

APPENDIX: GLOBAL ANALYSIS OF E.COLI RNA DEGRADOSOME FUNCTION

Introduction

Transcriptional regulation in bacteria has been under extensive study since the beginning of the molecular biology era. Much attention has been given on the post-transcription modification of mRNA during the past decade. These modifications include the binding of translational repressors/activators, formation of RNA secondary structures that inhibit turnove or ribosome binding, and the nucleolytic or phosphorylytic cleavage of mRNA. These modifications can activate/inactivate mRNA in terms of its function as a translational template, or stabilize/degrade mRNA Pulse-labeling and hybridization techniques have been used to measure the chemical half life of mRNA (based on the assumption that adding rifampicin blocks transcription). Microarray analyses have been employed to measure mRNA steady-state levels as well as half life of transcripts at the genome scale. Overall, these methods gave us limited information on the functional half life of mRNA *i.e.* how long an mRNA remains intact and accessible for translation. The assessment of mRNA functional half life is far more difficult and has relied on either an immunochemical or enzymatic assays.

A recently developed shotgun proteomic method, APEX (Absolute Protein Expression Index) can be used to evaluate the complete set of protein expression levels at the whole genome level (Lu, Vogel, Wang, Yao, & Marcotte, 2007).

Recent studies indicate that the assembled degradosome complex is necessary for normal mRNA degradation. Degradosome components functionally interact with each other during the decay of at least some RNAs in *E. coli*. There is an inverse relation between the mRNA decay rate and its cellular abundance. Previous work a showed that mRNAs encoded by genes with related functions commonly have similar half-lives (Bernstein, Khodursky, Lin, Lin-Chao, & Cohen, 2002). The DNA microarray study conducted by Bernstein *et al.* evaluated the steady-state level and decay of 4,289 E. coli mRNAs in strains carrying mutations in RNase E, PNPase, RhlB and enolase. The results indicated that certain mRNA decay involves the coordination from the degradosome components whereas other mRNA degradation is conducted or affected by individual components independently (Bernstein, Lin, Cohen, & Lin-Chao, 2004).

It is important to distinguish the chemical and functional half life of mRNA. If an mRNA is chemically degraded, it is not functional for translation, however, if an mRNA cannot be translated (*i.e.* functionally inactive) it doesn′t necessarily mean that it has been chemically degraded. To this end, we used APEX proteomic method to monitor the change in protein levels in strains carrying deletions in genes encoding degradosome components.

Materials and Methods

APEX METHOD, SAMPLE PREPARATION AND DATA ANALYSIS

Cells are grown at 30 °C in M9 media supplied with 0.2% tryptone, 0.2% glycerol, 1mM $MgSO_4$ and 0.0001% thiamine (For strains K10 and DF261, 40mM Succinate are added in the culture). Pellets are harvested at A_{600} of 0.6, resuspended in Lysis Buffer (25mM Tris HCl, 1mM EDTA pH7.5, before use, add 2.5mM DTT and 1x Roche Protease inhibitor) and lysed by French Press (20,000 psi, thrice). Soluble fractions after centrifugation (10,000g, 10min, at 4°C) are diluted into 4mg/ml. (Protein concentration determined by Nanodrop). Protein samples are denatured at 95 °C, 15min. After cool down to room temperature, trypsin solution (Sigma) was added at 1:50 (w/w). Digestions were carried out at 37 °C for 24hours. Sample after digestions were centrifuged through Micron YM-10 centrifuge device. The flow-through is subjected to APEX analysis according to Peng Lu *et al.*

CORRELATION OF MRNA AND PROTEIN USING PROG.PL

In order to compare microarray RNA data and APEX protein data, a PERL script is developed to match genes in RNA.txt file and genes in Protein.txt file, calculate the product of their associated values (log base 10(RNA/Protein fold change)), and return this product and the original RNA/Protein value in the output file result.txt. The script of this program is as follows:

```
# this program is called in xxx.pl fileRNA.txt fileProtien.txt
```

```
my $numArgs = @ARGV;


if($numArgs != 2){
        die("usage: perl xxx.pl path_file_RNA path_file_Protien");
}


my $fileRNA;
open($fileRNA,$ARGV[0]) || die("fileRNA can not be opened.\n");


my $fileProtien;
open($fileProtien,$ARGV[1]) || die("fileProtien can not be opened.\n");


my @geneName;
my @RNA;
my @tmp;


$tmp = <$fileRNA>;#just skip the first line
my @inputArray = <$fileRNA>; #read RNA file
my $length = @inputArray; #length of array
for (my $count=0 ; $count<$length ; $count++){
        @tmp = split(/\t/, @inputArray[$count]);
```

```
        @geneName[$count] = @tmp[0];
        @RNA[$count] = @tmp[1];
}
close($fileRNA);

$tmp = <$fileProtien>;
my @inputArray2 = <$fileProtien>;#read protien file
$length = @inputArray2;

my @geneName2;
my @protien;
for($count=0 ; $count<$length ; $count++){
        @tmp = split(/\t/, @inputArray2[$count]);
        @geneName2[$count] = @tmp[0];
        @protien[$count] = @tmp[1];
}
close($fileProtien);

#for each element in file RNA, find the corresponding record in file protien file according
to gene name. If the record is found, then compare the product of RNA and protien value
to 0. Finally, put the records into the output file.
```

```
my @correlation;
my @RNA2;
my @protien2;
my @geneName3;
my @index = 0;

$length = @geneName;
$length2 = @geneName2;
for(my $i=0 ; $i<$length ; $i++){
        for(my $j=0 ; $j<$length2 ; $j++){
                if(@geneName[$i] ne @geneName2[$j]){
                        next;
                }
                #find it
                @geneName3[$index] = @geneName[$i];

                my $z = @RNA[$i] * @protien[$j];
                @correlation[$index] = $z;

                @RNA2[$index] = @RNA[$i]*1;
                @protien2[$index] = @protien[$j];
```

```
                $index++;
                last;
        }
}

#write found records
($index > 0) || die("No correspingding records found.\n");

my $fileResult;
open($fileResult, ">result.txt") || die("Can not open output file");
print $fileResult ("gene\tcorrelation\tRNA\tprotien\n");#title

$length = @geneName3;

for($count=0 ; $count<$length ; $count++){
        print $fileResult ("@geneName[$count]\t@correlation[$count]\t@RNA2[$count]\t@protien2[$count]\n");
}
close($fileResult);
print("Done.\n");
```

Results and Discussion

PROTEINS IDENTIFIED IN APEX AND DATA VALIDATION.

Strains in Table 1 carrying degradosome component deletions were cultured in minimal media to log phase. Cells were collected, lysed by French press. Soluble fractions are completely digested by trypsin to generate peptide samples for Mass spectrometry analysis. About 1000 to 1500 proteins could be identified from each sample. (Table 1)

To evaluate the validity of the mass proteomic data we used two approaches: knowledge based validation and experimental validation.

First we checked the APEX values for proteins whose encoding gene had been deleted. In the YHC012 strain carrying the *Tn5::pnp* mutation, the amount of Pnpase protein was less than 1/10 of that detected in the parental strain (APEX fold change value, log (base 10) is -1.19, with significance z-score -14.06). Similar reductions in RhlB and Enolase protein abundance were (values) observed in the *rhlB* mutant and *eno* mutant respectively. In the *rne* truncation mutation it is well known that the RNase E protein, is overproduced and this was also reflect in the abundance of the protein by APEX.

Due to the limitation of available protein-specific antibodies, we tested several significantly increased or decreased proteins based on the availability of the antibody. GlmS protein shows an increase in YHC012 strain and decrease in SU02 strain compared to their wildtype N3433 strain. This was been confirmed by quantitative western blotting using polyclonal antibodies against GlmS. Similar experimental validation using anti-

CspE antibody and anti-OmpA antibody were also consistent with APEX values (data not shown).

Table A.1 Strains carrying mutations in the major degradosome components

Strain	Genotype	Number of proteins identified
N3433	lacZ, relA, spot1, thi1	1540
YHC012	N3433 except for *Tn5::pnp*	1008
SU02	N3433 except for *ΔrhlB*	1379
SH3208	his ΔtrpE5(λ)	1448
BZ453	SH3208 except for *rne* truncation	1372
K10	garB10, fhuA22, ompF627(T_2^R), fadL701(T_2^R), relA1, pit-10, spoT1, rrnB-2, mcrB1, creC510	1248
DF261	K10 except for *eno-2*	1322

PROTEINS AFFECTED BY TWO OR MORE DEGADOSOME MUTANTS

The abundance of several proteins was found to be affected in a similar manner in *pnp* and *rhlB* mutant strains. As a complex managing the decay of mRNA, one would expect the loss of coordination in mRNA decay will alter the protein levels accordingly. To our

surprise there were very few proteins whose level was affected in the same manner in all degradosome mutants. This data is summarized in Table 3.

Table A.2 Number of proteins which has significant abundance change in various degradosome component mutants (red: increase; green: decrease in mutants)

in 2 mutants	eno	Pnp	rhlB	rne
Eno		31	23	41
Pnp	20		278	73
rhlB	25	67		61
Rne	73	14	23	

in 3 mutants	increased	Decreased
eno pnp rhlB	17	8
eno pnp rne	10	5
rhlB rne eno	9	7
rhlB rne pnp	45	8
in all four mutants	7	3

CORRELATION BETWEEN MRNA AND PROTEIN LEVELS

Bernstein *et al.* used microarrays to identify transcripts that are over or under represented in the four degradosome mutants discussed above. Only 286 transcripts showed similar changes in all four mutations (Bernstein, Lin, Cohen, & Lin-Chao, 2004). They also measured mRNA half life in various strains and obtained mRNA half lives for about 2000 transcripts in these mutant strains.

We sought to determine whether there is a correlation between changes in mRNA abundance and protein abundance. We developed a perl program to compare the APEX protein data with the earlier RNA transcriptional profile data. In this program we compared the mRNA steady state level change with the protein level change by calculating the product of the respective fold-changes (log base 10 value). If the product>0, it means the RNA level and protein level are changing in a coordinated fashion (both increase/decrease) and *vice versa*. The cut-off of protein folds change data were 1.5x and 0.67x fold-change for increased or decreased abundances respectively. The results are summarized in Table 3.

Table A.3. Comparisons of mRNA and Protein.

strains	correlation	consistent	inconsistent	Total
eno	0.446328	158	196	354
pnp	0.567358	219	167	386
rhlB	0.572539	221	137	386
rne	0.569767	196	148	344

Several facts contribute to the existence of irrelevancy between the mRNA and protein. First microarray analysis measures the chemical half life, as stated above; transcripts that quickly adapted to a translational inactive structure can have a long chemical half-life and show high abundance chemically but have a short functional half life and cannot be translated. Second, the various mutants used in this study may affect rates of protein degradation.

Further data analysis regarding to the details of the pathways to which this correlated (or not correlated) genes belongs will provide more information on the significance of RNA degrasome as a means of gene expression control. Moreover, incorporation of RNase E inhibitors RraA and RraB in a similar study will be very useful in elucidating the function of these protein inhibitors. Of note, the previous study done by our group has already established the transcriptional profile under conditions of over-expressing RraA/RraB (Gao et al. 2006).

Bibliography

Baker, K., Mackman, N., Jackson, M., & Holland, I. B. (1987). Role of SecA and SecY in protein export as revealed by studies of TonA assembly into the outer membrane of Escherichia coli. *Journal of molecular biology*, *198*(4), 693-703.

Bardwell, J. C., McGovern, K., & Beckwith, J. (1991). Identification of a protein required for disulfide bond formation in vivo. *Cell*, *67*(3), 581-9.

Bernhardt, T. G., & de Boer, P. A. (2004). Screening for synthetic lethal mutants in Escherichia coli and identification of EnvC (YibP) as a periplasmic septal ring factor with murein hydrolase activity. *Molecular microbiology*, *52*(5), 1255-69.

Bernstein, J. A., Khodursky, A. B., Lin, P., Lin-Chao, S., & Cohen, S. N. (2002). Global analysis of mRNA decay and abundance in Escherichia coli at single-gene resolution using two-color fluorescent DNA microarrays. *Proceedings of the National Academy of Sciences of the United States of America*, *99*(15), 9697-702.

Bernstein, J. A., Lin, P., Cohen, S. N., & Lin-Chao, S. (2004). Global analysis of Escherichia coli RNA degradosome function using DNA microarrays. *Proceedings of the National Academy of Sciences of the United States of America*, *101*(9), 2758-63.

Bessette, P. H., Qiu, J., Bardwell, J. C., Swartz, J. R., & Georgiou, G. (2001). Effect of sequences of the active-site dipeptides of DsbA and DsbC on in vivo folding of multidisulfide proteins in Escherichia coli. *Journal of bacteriology*, *183*(3), 980-8.

Bouvet, P., & Belasco, J. G. (1992). Control of RNase E-mediated RNA degradation by 5′-terminal base pairing in E. coli. *Nature*, *360*(6403), 488-91.

Briani, F., Del Favero, M., Capizzuto, R., Consonni, C., Zangrossi, S., Greco, C., et al. (2007). Genetic analysis of polynucleotide phosphorylase structure and functions. *Biochimie*, *89*(1), 145-57.

Butland, G., Peregrín-Alvarez, J. M., Li, J., Yang, W., Yang, X., Canadien, V., et al. (2005). Interaction network containing conserved and essential protein complexes in Escherichia coli. *Nature*, *433*(7025), 531-7.

Callaghan, A. J., Aurikko, J. P., Ilag, L. L., Günter Grossmann, J., Chandran, V., Kühnel, K., et al. (2004). Studies of the RNA degradosome-organizing domain of the Escherichia coli ribonuclease RNase E. *Journal of molecular biology*, *340*(5), 965-79.

Callaghan, A. J., Grossmann, J. G., Redko, Y. U., Ilag, L. L., Moncrieffe, M. C., Symmons, M. F., et al. (2003). Quaternary structure and catalytic activity of the Escherichia coli ribonuclease E amino-terminal catalytic domain. *Biochemistry*, *42*(47), 13848-55.

Callaghan, A. J., Marcaida, M. J., Stead, J. A., McDowall, K. J., Scott, W. G., Luisi, B. F., et al. (2005). Structure of Escherichia coli RNase E catalytic domain and implications for RNA turnover. *Nature*, *437*(7062), 1187-91.

Carpousis, A. J., Luisi, B. F., & McDowall, K. J. (2009). *Molecular Biology of RNA Processing and Decay in Prokaryotes*. *Progress in molecular biology and translational science*, Progress in Molecular Biology and Translational Science Vol. 85, pp. 91-135

Cartier, G., Lorieux, F., Allemand, F., Dreyfus, M., & Bizebard, T. (2010). Cold adaptation in DEAD-box proteins. *Biochemistry*, *49*(12), 2636-46.

Caruthers, J. M., Feng, Y., McKay, D. B., & Cohen, S. N. (2006). Retention of core catalytic functions by a conserved minimal ribonuclease E peptide that lacks the domain required for tetramer formation. *The Journal of biological chemistry*, *281*(37), 27046-51.

Carzaniga, T., Briani, F., Zangrossi, S., Merlino, G., Marchi, P., Dehò, G., et al. (2009). Autogenous regulation of Escherichia coli polynucleotide phosphorylase expression revisited. *Journal of bacteriology*, *191*(6), 1738-48.

Chandran, V., & Luisi, B. F. (2006). Recognition of enolase in the Escherichia coli RNA degradosome. *Journal of molecular biology*, *358*(1), 8-15.

Chandran, V., Poljak, L., Vanzo, N. F., Leroy, A., Miguel, R. N., Fernandez-Recio, J., et al. (2007). Recognition and cooperation between the ATP-dependent RNA helicase RhlB and ribonuclease RNase E. *Journal of molecular biology*, *367*(1), 113-32.

Collins, J. A., Irnov, I., Baker, S., & Winkler, W. C. (2007). Mechanism of mRNA destabilization by the glmS ribozyme. *Genes & development*, *21*(24), 3356-68.

Cormack, R. S., Genereaux, J. L., & Mackie, G. A. (1993). RNase E activity is conferred by a single polypeptide: overexpression, purification, and properties of the ams/rne/hmp1 gene product. *Proceedings of the National Academy of Sciences of the United States of America*, *90*(19), 9006-10

Deana, A.Celesnik, H., & Belasco, J. G. (2008). The bacterial enzyme RppH triggers messenger RNA degradation by 5′ pyrophosphate removal. *Nature*, *451*(7176), 355-8.

Del Favero, M., Mazzantini, E., Briani, F., Zangrossi, S., Tortora, P., Dehò, G., et al. (2008). Regulation of Escherichia coli polynucleotide phosphorylase by ATP. *The Journal of biological chemistry*, *283*(41), 27355-9.

Denisot, M. A., Le Goffic, F., & Badet, B. (1991). Glucosamine-6-phosphate synthase from Escherichia coli yields two proteins upon limited proteolysis: identification of the glutamine amidohydrolase and 2R ketose/aldose isomerase-bearing domains based on their biochemical properties. *Archives of biochemistry and biophysics*, *288*(1), 225-30.

Diwa, A. A., & Belasco, J. G. (2002). Critical features of a conserved RNA stem-loop important for feedback regulation of RNase E synthesis. *The Journal of biological chemistry*, *277*(23), 20415-22.

Diwa, A., Bricker, A. L., Jain, C., & Belasco, J. G. (2000). An evolutionarily conserved RNA stem-loop functions as a sensor that directs feedback regulation of RNase E gene expression. *Genes & development*, *14*(10), 1249-60.

Eguchi, Y., & Tomizawa, J. (1991). Complexes formed by complementary RNA stem-loops Their formations, structures and interaction with ColE1 Rom protein. *Journal of Molecular Biology*, *220*(4), 831-842.

Faulkner, M. J., Veeravalli, K., Gon, S., Georgiou, G., & Beckwith, J. (2008). Functional plasticity of a peroxidase allows evolution of diverse disulfide-reducing pathways. *Proceedings of the National Academy of Sciences of the United States of America*, *105*(18), 6735-40.

Gao, J., Lee, K., Zhao, M., Qiu, J., Zhan, X., Saxena, A., et al. (2006). Differential modulation of E. coli mRNA abundance by inhibitory proteins that alter the composition of the degradosome. *Molecular microbiology*, *61*(2), 394-406.

Garrey, S. M., Blech, M., Riffell, J. L., Hankins, J. S., Stickney, L. M., Diver, M., et al. (2009). Substrate binding and active site residues in RNases E and G: role of the 5′-sensor. *The Journal of biological chemistry*, *284*(46), 31843-50.

Godefroy-Colburn, T.; Grunenberg-Manago, M. (1972). *The Enzymes 3rd. Ed.* (P. Boyer) (pp. 533-574).

Gorna, M. W., Pietras, Z., Tsai, Y., Callaghan, A. J., Hernandez, H., Robinson, C. V., et al. (2010). The regulatory protein RraA modulates RNA-binding and helicase activities of the E. coli RNA degradosome. *RNA (New York, N.Y.)*, *16*(3), 553-62.

Grigorova, I. L., Chaba, R., Zhong, H. J., Alba, B. M., Rhodius, V., Herman, C., et al. (2004). Fine-tuning of the Escherichia coli sigmaE envelope stress response relies on multiple mechanisms to inhibit signal-independent proteolysis of the transmembrane anti-sigma factor, RseA. *Genes & development*, *18*(21), 2686-97.

Guzman, L. M., Belin, D., Carson, M. J., & Beckwith, J. (1995). Tight regulation, modulation, and high-level expression by vectors containing the arabinose PBAD promoter. *Journal of bacteriology*, *177*(14), 4121-30

Haldimann, A., Daniels, L. L., & Wanner, B. L. (1998). Use of new methods for construction of tightly regulated arabinose and rhamnose promoter fusions in studies of the Escherichia coli phosphate regulon. *Journal of bacteriology*, *180*(5), 1277-86.

Iost, I., & Dreyfus, M. (2006). DEAD-box RNA helicases in Escherichia coli. *Nucleic acids research*, *34*(15), 4189-97.

Jain, C., & Belasco, J. G. (1995). RNase E autoregulates its synthesis by controlling the degradation rate of its own mRNA in Escherichia coli: unusual sensitivity of the rne transcript to RNase E activity. *Genes & Development*, *9*(1), 84-96.

Jiang, X., & Belasco, J. G. (2004). Catalytic activation of multimeric RNase E and RNase G by 5′-monophosphorylated RNA. *Proceedings of the National Academy of Sciences of the United States of America*, *101*(25), 9211-6.

Joanny, G., Le Derout, J., Bréchemier-Baey, D., Labas, V., Vinh, J., Régnier, P., et al. (2007). Polyadenylation of a functional mRNA controls gene expression in Escherichia coli. *Nucleic acids research*, *35*(8), 2494-502.

Jourdan, S. S., & McDowall, K. J. (2008). Sensing of 5′ monophosphate by Escherichia coli RNase G can significantly enhance association with RNA and stimulate the decay of functional mRNA transcripts in vivo. *Molecular microbiology*, *67*(1), 102-15.

Jourdan, S. S., Kime, L., & McDowall, K. J. (2010). The sequence of sites recognised by a member of the RNase E/G family can control the maximal rate of cleavage, while a 5′-monophosphorylated end appears to function cooperatively in mediating RNA binding. *Biochemical and biophysical research communications*, *391*(1), 879-83.

Kaberdin, V. R. (2003). Probing the substrate specificity of Escherichia coli RNase E using a novel oligonucleotide-based assay. *Nucleic acids research*, *31*(16), 4710-6.

Kaberdin, V. R., Chao, Y., & Lin-Chao, S. (1996). RNase E Cleaves at Multiple Sites in Bubble Regions of RNA I Stem Loops Yielding Products That Dissociate Differentially from the Enzyme. *Journal of Biological Chemistry*, *271*(22), 13103-13109.

Kalamorz, F., Reichenbach, B., März, W., Rak, B., & Görke, B. (2007). Feedback control of glucosamine-6-phosphate synthase GlmS expression depends on the small RNA GlmZ and involves the novel protein YhbJ in Escherichia coli. *Molecular microbiology*, *65*(6), 1518-33.

Khemici, V., Poljak, L., Luisi, B. F., & Carpousis, A. J. (2008). The RNase E of Escherichia coli is a membrane-binding protein. *Molecular microbiology*, *70*(4), 799-813.

Khodursky, A. B., Peter, B. J., Cozzarelli, N. R., Botstein, D., Brown, P. O., Yanofsky, C., et al. (2000). DNA microarray analysis of gene expression in response to physiological and genetic changes that affect tryptophan metabolism in Escherichia coli. *Proceedings of the National Academy of Sciences of the United States of America*, *97*(22), 12170-5.

Kime, L., Jourdan, S. S., Stead, J. A., Hidalgo-Sastre, A., & McDowall, K. J. (2009). Rapid cleavage of RNA by RNase E in the absence of 5′-monophosphate stimulation. *Molecular microbiology*, *76*(3) 590-604.

Koslover, D. J., Callaghan, A. J., Marcaida, M. J., Garman, E. F., Martick, M., Scott, W. G., et al. (2008). The crystal structure of the Escherichia coli RNase E apoprotein and a mechanism for RNA degradation. *Structure (London, England : 1993)*, *16*(8), 1238-44.

Krin, E., Laurent-Winter, C., Bertin, P. N., Danchin, A., & Kolb, A. (2003). Transcription Regulation Coupling of the Divergent argG and metY Promoters in Escherichia coli K-12. *Journal of Bacteriology*, *185*(10), 3139-3146.

Kühnel, K., & Luisi, B. F. (2001). Crystal structure of the Escherichia coli RNA degradosome component enolase. *Journal of molecular biology*, *313*(3), 583-92.

Lacatena, R. M., & Cesareni, G. (1981). Base pairing of RNA I with its complementary sequence in the primer precursor inhibits ColE1 replication. *Nature*, *294*(5842), 623-626.

Lee, A. J., & Crothers, D. M. (1998). The solution structure of an RNA loop–loop complex: the ColE1 inverted loop sequence. *Structure*, *6*(8), 993-1007.

Lee, K., Zhan, X., Gao, J., Qiu, J., Feng, Y., Meganathan, R., et al. (2003). RraAa Protein Inhibitor of RNase E Activity that Globally Modulates RNA Abundance in E. coli. *Cell*, *114*(5), 623-634.

Lee, M., Yeom, J., Sim, S., Ahn, S., & Lee, K. (2009). Effects of Escherichia coli RraA orthologs of Vibrio vulnificus on the ribonucleolytic activity of RNase E in vivo. *Current microbiology*, *58*(4), 349-53.

Li, Z., & Deutscher, M. P. (2002). RNase E plays an essential role in the maturation of Escherichia coli tRNA precursors. *RNA (New York, N.Y.)*, *8*(1), 97-109.

Lin, P., & Lin-Chao, S. (2005). RhlB helicase rather than enolase is the beta-subunit of the Escherichia coli polynucleotide phosphorylase (PNPase)-exoribonucleolytic complex. *Proceedings of the National Academy of Sciences of the United States of America*, *102*(46), 16590-5.

Liou, G., Chang, H., Lin, C., & Lin-Chao, S. (2002). DEAD box RhlB RNA helicase physically associates with exoribonuclease PNPase to degrade double-stranded RNA independent of the degradosome-assembling region of RNase E. *The Journal of biological chemistry*, *277*(43), 41157-62.

Littauer, U.Z.; Soreq, H. (1982). *The Enzymes, 3rd. Ed.* (P. D. Boyer) (pp. 517-553). Academic Press.

Lu, P., Vogel, C., Wang, R., Yao, X., & Marcotte, E. M. (2007). Absolute protein expression profiling estimates the relative contributions of transcriptional and translational regulation. *Nature biotechnology*, *25*(1), 117-24.

Mackie, G. A. (1998). Ribonuclease E is a 5′-end-dependent endonuclease. *Nature*, *395*(6703), 720-3.

Makarova, K. S., Mironov, A. A., & Gelfand, M. S. (2001). Conservation of the binding site for the arginine repressor in all bacterial lineages. *Genome biology*, *2*(4), RESEARCH0013

Maria C. Ow, Qi Liu,† Bijoy K. Mohanty, M. E., & Andrew, V. F. (2002). RNase E levels in Escherichia coli are controlled by a complex regulatory system that involves transcription of the rne gene from three promoters. *Molecular Microbiology*, *43*(1), 159-171.

Meganathan, R. (1996). *Escherichia coli and Salmonella: cellular and molecular biology*. Progress in Molecular Biology and Translational Science (Vol. 85). American Society for Microbiology.

Milewski, S. (2002). Glucosamine-6-phosphate synthase--the multi-facets enzyme. *Biochimica et biophysica acta*, *1597*(2), 173-92.

Miller, J. H. (1972). *Experiments in molecular genetics*. Cold Spring Harbor Laboratory Press.

Miller, J. H. (1992). *A short course in bacterial genetics: a laboratory manual and handbook for Escherichia coli and related bacteria.*. Cold Spring Harbor Laboratory Press.

Misra, T. K., & Apirion, D. (1979). RNase E, an RNA processing enzyme from Escherichia coli. *The Journal of biological chemistry*, *254*(21), 11154-9.

Mudd, E. A., & Higgins, C. F. (1993). Escherichia coli endoribonuclease RNase E: autoregulation of expression and site-specific cleavage of mRNA. *Molecular microbiology*, *9*(3), 557-68

Namboori, S. C., & Graham, D. E. (2008). Enzymatic analysis of uridine diphosphate N-acetyl-D-glucosamine. *Analytical biochemistry*, *381*(1), 94-100.

Nishio, S., & Itoh, T. (2009). Arginine-rich RNA binding domain and protein scaffold domain of RNase E are important for degradation of RNAI but not for that of the Rep mRNA of the ColE2 plasmid. *Plasmid*, *62*(2), 83-7.

Nurmohamed, S., Vaidialingam, B., Callaghan, A. J., & Luisi, B. F. (2009). Crystal structure of Escherichia coli polynucleotide phosphorylase core bound to RNase E, RNA and manganese: implications for catalytic mechanism and RNA degradosome assembly. *Journal of molecular biology*, *389*(1), 17-33.

Ow, M. C., & Kushner, S. R. (2002). Initiation of tRNA maturation by RNase E is essential for cell viability in E. coli. *Genes & development*, *16*(9), 1102-15.

Ow, M. C., Liu, Q., & Kushner, S. R. (2000). Analysis of mRNA decay and rRNA processing in Escherichia coli in the absence of RNase E-based degradosome assembly. *Molecular Microbiology*, *38*(4), 854-866.

Perwez, T., Hami, D., Maples, V. F., Min, Z., Wang, B., Kushner, S. R., et al. (2008). Intragenic suppressors of temperature-sensitive rne mutations lead to the

dissociation of RNase E activity on mRNA and tRNA substrates in Escherichia coli. *Nucleic acids research*, *36*(16), 5306-18.

Podkovyrov, S. M., & Larson, T. J. (1995). A new vector-host system for construction of lacZ transcriptional fusions where only low-level gene expression is desirable. *Gene*, *156*(1), 151-2.

Ramelot, T. A., Ni, S., Goldsmith-fischman, S., Cort, J. R., Honig, B., Kennedy, M. A., et al. (2003). Solution structure of Vibrio cholerae protein VC0424 : A variation of the ferredoxin-like fold. *Protein Science*, *12*(509), 1556-1561.

Redko, Y., Tock, M. R., Adams, C. J., Kaberdin, V. R., Grasby, J. A., McDowall, K. J., et al. (2003). Determination of the catalytic parameters of the N-terminal half of Escherichia coli ribonuclease E and the identification of critical functional groups in RNA substrates. *The Journal of biological chemistry*, *278*(45), 44001-8.

Reed, G. H., Poyner, R. R., Larsen, T. M., Wedekind, J. E., & Rayment, I. (1996). Structural and mechanistic studies of enolase. *Current opinion in structural biology*, *6*(6), 736-43.

Reichenbach, B., Maes, A., Kalamorz, F., Hajnsdorf, E., & Görke, B. (2008). The small RNA GlmY acts upstream of the sRNA GlmZ in the activation of glmS expression and is subject to regulation by polyadenylation in Escherichia coli. *Nucleic acids research*, *36*(8), 2570-80.

Schubert, M., Edge, R. E., Lario, P., Cook, M. A., Strynadka, N. C., Mackie, G. A., et al. (2004). Structural characterization of the RNase E S1 domain and identification of its oligonucleotide-binding and dimerization interfaces. *Journal of molecular biology*, *341*(1), 37-54.

Shin, E., Go, H., Yeom, J., Won, M., Bae, J., Han, S. H., et al. (2008). Identification of amino acid residues in the catalytic domain of RNase E essential for survival of Escherichia coli: functional analysis of DNase I subdomain. *Genetics*, *179*(4), 1871-9.

Shineberg, B., & Young, I. G. (1976). Biosynthesis of bacterial menaquinones: the membrane-associated 1,4-dihydroxy-2-naphthoate octaprenyltransferase of Escherichia coli. *Biochemistry*, *15*(13), 2754-8.

Simons, R. W., Houman, F., & Kleckner, N. (1987). Improved single and multicopy lac-based cloning vectors for protein and operon fusions. *Gene*, *53*(1), 85-96.

Singh, D., Chang, S., Lin, P., Averina, O. V., Kaberdin, V. R., Lin-Chao, S., et al. (2009). Regulation of ribonuclease E activity by the L4 ribosomal protein of Escherichia coli. *Proceedings of the National Academy of Sciences of the United States of America*, *106*(3), 864-9.

Strauch, K. L. (1988). An Escherichia coli Mutation Preventing Degradation of Abnormal Periplasmic Proteins. *Proceedings of the National Academy of Sciences*, *85*(5), 1576-1580

Taghbalout, A., & Rothfield, L. (2007). RNaseE and the other constituents of the RNA degradosome are components of the bacterial cytoskeleton. *Proceedings of the National Academy of Sciences of the United States of America*, *104*(5), 1667-72.

Taraseviciene, Laimute, Bjork, Glenn R. And Uhlin, B. E. (1995). Evidence for an RNA Binding Region in the Escherichia coli processing Endoribonuclease RNase E. *Journal of Biological Chemistry*, *270*(44), 26391-26398.

Teplyakov, A., Obmolova, G., Badet, B., & Badet-Denisot, M. A. (2001). Channeling of ammonia in glucosamine-6-phosphate synthase. *Journal of molecular biology*, *313*(5), 1093-102.

Vanzo, N. F., Li, Y. S., Py, B., Blum, E., Higgins, C. F., Raynal, L. C., et al. (1998). Ribonuclease E organizes the protein interactions in the Escherichia coli RNA degradosome. *Genes & Development*, *12*(17), 2770-2781.

Worrall, J. A., Górna, M., Crump, N. T., Phillips, L. G., Tuck, A. C., Price, A. J., et al. (2008). Reconstitution and analysis of the multienzyme Escherichia coli RNA degradosome. *Journal of molecular biology*, *382*(4), 870-83.

Worrall, J. A., Howe, F. S., McKay, A. R., Robinson, C. V., & Luisi, B. F. (2008). Allosteric activation of the ATPase activity of the Escherichia coli RhlB RNA helicase. *The Journal of biological chemistry*, *283*(9), 5567-76.

Wu, J., Jiang, Z., Liu, M., Gong, X., Wu, S., Burns, C. M., et al. (2009). Polynucleotide phosphorylase protects Escherichia coli against oxidative stress. *Biochemistry*, *48*(9), 2012-20.

Yeom, J., Shin, E., Go, H., Sim, S., Seong, M., Lee, K., et al. (2008). Functional implications of the conserved action of regulators of ribonuclease activity. *Journal of microbiology and biotechnology*, *18*(8), 1353-6.

Zeller, M., Csanadi, A., Miczak, A., Rose, T., Bizebard, T., Kaberdin, V. R., et al. (2007). Quaternary structure and biochemical properties of mycobacterial RNase E/G. *The Biochemical journal*, *403*(1), 207-15.

Zhan, X., Gao, J., Jain, C., Cieslewicz, M. J., Swartz, J. R., Georgiou, G., et al. (2004). Genetic Analysis of Disulfide Isomerization in Escherichia coli: Expression of DsbC Is Modulated by RNase E-Dependent mRNA Processing. *Journal of Bacteriology*, *186*(3), 654-660.

Zhang, H., Zhou, Y., Bao, H., & Liu, H. (2006). Vi antigen biosynthesis in Salmonella typhi: characterization of UDP-N-acetylglucosamine C-6 dehydrogenase (TviB) and UDP-N-acetylglucosaminuronic acid C-4 epimerase (TviC). *Biochemistry*, *45*(26), 8163-73.

Zhao, M., Zhou, L., Kawarasaki, Y., & Georgiou, G. (2006). Regulation of RraA, a protein inhibitor of RNase E-mediated RNA decay. *Journal of bacteriology*, *188*(9), 3257-63.

Zhou, L. Zhao M. Georgiou G. (2009). Transcriptional regulation of *Eshericia coli* gene rraB, encoding a protein inhibitor of RNase E. *Journal of bacteriology*, *191*(21), 6665-74.

Vita

Li Zhou was born in Shanxi, China on November 10, 1982, the daughter of Feng Zhao and Xueliang Zhou. She received a Bachelor of Science degree in biological science and technology from Tsinghua University in Beijing, China, in 2004. In the autumn of 2004 she enrolled in the Graduate of School at the University of Texas at Austin.

Permanent address: No. 48 Yanghao Street, Yuci District, Jinzhong City, Shanxi, China 030600

This dissertation was typed by Li Zhou.